

Digital twin enabled sustainable urban road planning

Feng Jiang^a, Ling Ma^{a,*}, Tim Broyd^a, Weiya Chen^b, Hanbin Luo^b

^a The Bartlett School of Sustainable Construction, University College London, London WC1E 6BT, UK

^b School of Civil Engineering and Mechanics, Huazhong University of Science and Technology, Wuhan 430074, China



ARTICLE INFO

Keywords:

Sustainable urban road planning
Digital twin
MCDM
Alignment selection
Building demolition
Land use
Traffic congestion
Driving route selection habits
Air quality
Noise

ABSTRACT

Sustainable urban road planning should endeavor to meet current and future traffic-related demands and achieve financial, environmental, and social benefits, which is a complex and interdisciplinary issue that needs to consider various factors and data. Multi-criteria decision making (MCDM) can provide reasonable solutions, and some existing studies integrated MCDM with geographic information system (GIS) technology. This paper presents an urban road planning approach based on digital twin (DT), MCDM, and GIS called DT-MCDM-GIS framework. DT can digitalize the physical world to provide various data for the whole process; MCDM can provide criteria and evaluation methods; GIS can provide an integrated environment for analysis. Building demolition and land use, traffic congestion, driving route selection habits, air quality, and noise are all considered in the framework for urban road planning. The proposed approach can provide a functional, economic, people-friendly, eco-friendly urban road planning scheme considering new road construction and existing old road widening to alleviate traffic congestion and provide an alternative route for drivers that conforms to their habits.

1. Introduction

Sustainable urban road planning strives to cope with current and future traffic-related demands and achieve financial, environmental, and social goals (Addanki & Venkataraman, 2017; Ma & Peng, 2021). It is a complex and interdisciplinary issue that needs to consider many factors, including engineering, transportation, economic, policy, environmental, and social factors (Gipps, Gu, Held, & Barnett, 2001). However, with the progress of urbanization, everything seems to worsen. Cities are becoming densely populated, and severe traffic congestion frequently occurs (Pucher, Peng, Mittal, Zhu, & Koratty-swaroopam, 2007). In addition, functional urban areas such as commercial areas, residential areas, industrial areas, green areas, etc., are set up, available urban land decreases, and the houses' price increases (Ehrlich, Hilber, & Schöni, 2018). In the city, air quality reduces and noise increases due to the vehicles, factories, commercial activities, etc. (Kabisch & Haase, 2013). Urban planning needs to alleviate these problems, and urban road planning is an essential part of it.

On the one hand, urban road planning aims to meet functional requirements from the citizens. On the other hand, urban road planning needs to consider the economic constraints, a city's limited remaining space for construction, and environmental requirements. Considering

various demands and constraints, sustainable urban road planning endeavours to propose functional, economical, people-friendly, eco-friendly schemes.

Multi-Criteria Decision Making (MCDM) and Geographical Information Systems (GIS) are used in some studies to assist in urban road planning (Ouma, Yabann, Kirichu, & Tateishi, 2014), and Analytic Hierarchy Process (AHP) is one of the most widely used MCDM methods (Saaty, 1977). Using MCDM methods, most existing studies only consider road planning for newly built roads. However, with the continuous development of cities, the increase in the number of buildings, and the expansion of road networks, less and less remaining space is available for new roads construction. Therefore, when planning roads, designers need to balance the limited space in the city and the ever-increasing traffic demands of citizens. Furthermore, road widening and new road construction should be considered when planning roads and designers endeavor to reduce building demolition and road land use with high cost (Brahmantoro, Hidayat, & Sebayang, 2019). Thus, environment and surroundings, existing road networks, other existing related data play an essential role in urban road planning.

Digitalizing and interpreting the information in the physical world, including geometric and non-geometric information, is essential for road planning. The digital twin (DT) paradigm can provide a feasible solution

* Corresponding author at: The Bartlett School of Sustainable Construction, University College London, 1-19 Torrington Place, London WC1E 7HB, UK.

E-mail addresses: feng.jiang.20@ucl.ac.uk (F. Jiang), l.ma@ucl.ac.uk (L. Ma), tim.broyd@ucl.ac.uk (T. Broyd), weiya_chen@hust.edu.cn (W. Chen), luohbcem@hust.edu.cn (H. Luo).

to this issue. DT is a set of virtual information constructs that fully describes a potential or actual physical manufactured product from the micro atomic level to the macro geometrical level. Any information obtained from inspecting a physically manufactured product can be obtained from its DT at its optimum (Grieves & Vickers, 2016). Many sectors have employed digital twin to realize many applications, especially in the manufacturing (Leng et al., 2021) and aerospace industry (Liu et al., 2021), and DT has expanded to the construction sector, including the design stage, construction stage, and operation and maintenance stage (Jiang, Ma, Broyd, & Chen, 2021). Digital twins of the existing related projects, surroundings and environment, can be established to assist in decision making and designing (e.g. digital twin city) (Shahat, Hyun, & Yeom, 2021). By collecting data from the physical world and parsing data into understandable expressions, DT can assist in complex and sustainable urban road planning considering various factors.

This study aims to provide planners with a sustainable urban road planning approach which focuses on interpreting various data from multiple sources in the physical world into a digital expression called cost map based on DT, MCDM and GIS to assist in urban road planning, considering both new road construction and existing old road widening. In this paper, several factors are considered: building demolition and land use, traffic congestion, driving route selection habits, air quality, and noise.

This paper begins with a systematic review in [Section 2](#) Reference source not found. Next, the proposed approach will be introduced in detail in [Section 3](#). Then, the proposed approach is employed in an area in London which will be introduced in [Section 4](#). Finally, [Section 5](#) is the discussion, and [Section 6](#) is the conclusion of this paper.

2. Literature review

2.1. Urban road planning

Urban road planning aims to improve roads' accessibility, functionality, and economy according to various data types from multiple sources. Many studies have proposed various methods for urban road planning. First, from the macroscopical perspective of the overall economy and policy of road planning, Zhang (2016) analyzed the development laws and characteristics of urban logistics structure from a theoretical perspective to understand the status and role of logistics network space in urban planning. Urban road planning and design was the focus of the research. Ng, Law, Jakarni, and Kulanthayan (2018) employed a fixed-effects panel linear regression analysis on a panel of 60 countries from 1980 to 2010 to reveal how much investment was appropriate for various road types to facilitate urban growth at different levels of urbanization and how the development of various road types could promote export-led urban growth. Ma and Peng (2021) employed the with-without comparison principle and aboveground-underground comparison principle to determine nine sustainability-oriented benefits in the operation of complex underground roads, including intrinsic benefits and specific benefits. Second, from the perspective of the geometric information of road networks and travelling time, Hou, Maruyama, Hirota, and Kato (2009) proposed a road network optimization framework directed by unblocked reliability for given network topology and inelastic demand with stochastic user equilibrium. The proposed optimization framework could improve the road network to its highest possible reliability level with a minimum scale of road network expansion. Wang and Chen (2016) proposed a hybrid algorithm based on particle swarms and ant colonies to optimize travel routes in cities, improving travel efficiency and accuracy and providing a reliable basis for optimizing urban roads and cities. Third, for urban road planning, improving the road service capabilities is often concerned, such as reducing traffic congestion and improving traffic-related functions. Chen, Wang, and Tian (2019) presented a visualization model based on graph theory's self-organizing feature map neural network. They

analyzed traffic data throughout the life cycle, sorted out the collection, analysis, discovery, and application levels of traffic data, and employed big data technology to guide urban traffic planning, construction, management, operation, and decision support. Lanqin (2020) proposed a spatio-temporal analysis approach of intelligent urban road planning congestion based on the spectral clustering algorithm of big data mining, which could shorten the time gap and improve the effectiveness. Similarly, pedestrians are also an important factor for road planning. Scoppa, Bawazir, and Alawadi (2018) analyzed the superblocks' walkability and the role of narrow alleys between plots to provide efficient and direct pedestrian routes, where the efficiency was quantified using pedestrian route directness and referred to a measure that captures the ability of the layout to provide direct routes between origins and destinations. The research could contribute to policy-making for urban design and urban design theory for street layouts with narrow alleyways between plots. Fourth, urban road planning also considers other factors, such as points of interest (POI), pollutants, noise emissions, etc. Through spatial modeling in urban agglomerations, Zeng et al. (2019) explored the spatial spillover impact of infrastructure networks on urbanization in the two hypotheses based on road networks and points of interest (POI), respectively. Fernandes et al. (2020) compared various suburban roundabouts in traffic performance, pollutants, and noise emissions through comprehensive empirical evaluation. They proposed a method to quantify the performance of suburban roundabout layouts. Meng and Shao (2011) proposed a multi-stage and multi-attribute model based on Data Envelopment Analysis and TOPSIS to improve urban road planning and construction availability. Accordingly, the sequence of urban road construction could be obtained. Khayamim, Shetab-Boushehrb, Hosseiniinasab, and Karimi (2020) proposed a method to simultaneously select and time urban traffic projects based on a two-level mathematical programming model and a two-stage hybrid solution procedure. The proposed method could consider a large transportation network with many candidate projects and choose and schedule projects based on sustainable development. Moreover, some road planning considers special periods. Francini, Gaudio, Palermo, and Viapiana (2020) presented a performance-based approach to identify strategic road infrastructures at the municipal level to know which roads remained available in case of emergency according to Risk Index integrating multi-criteria techniques, GIS, fuzzy logic, and structural vulnerability analysis.

2.2. Road planning based on MCDM and GIS

Hybrid MCDM – GIS methods are employed to plan roads in some studies to provide optimal road alignment according to various factors. For example, Grossardt, Bailey, and Brumm (2001) presented using the analytical minimum impedance surface (AMIS) method for road planning. The characteristic of AMIS is that the input of stakeholders is structurally integrated into the GIS-based hybrid hierarchical analysis process. Beukes, Vanderschuren, Zuideest, Brussel, and van Maarseveen (2013) proposed the COSMA method, which uses contextual information to formulate road infrastructure recommendations to improve road design using GIS and spatial multi-criteria analysis considering land use and socioeconomic environmental, and transportation information. Ouma et al. (2014) modified the traditional AHP method to fuzzy AHP to find the optimal bypass route for Eldoret, Kenya, using GIS. Yakar and Celik (2014) proposed a three-stage model based on MCDM and GIS for highway route selection. Singh, Singh, and Singh (2019) proposed a method to identify and select road schemes using GIS and fuzzy AHP. Spatial multi-criteria decision analysis was employed to determine the best alignment considering environmental, social, economic and technological spatial data and other criteria. Hosseini, Moghadasi, and Fallah (2019) presented a method to design forest roads using GIS and satellite data based on multipurpose forestry. The study employed the multi-criteria evaluation method based on fuzzy logic to evaluate the potential of land area for a road network.

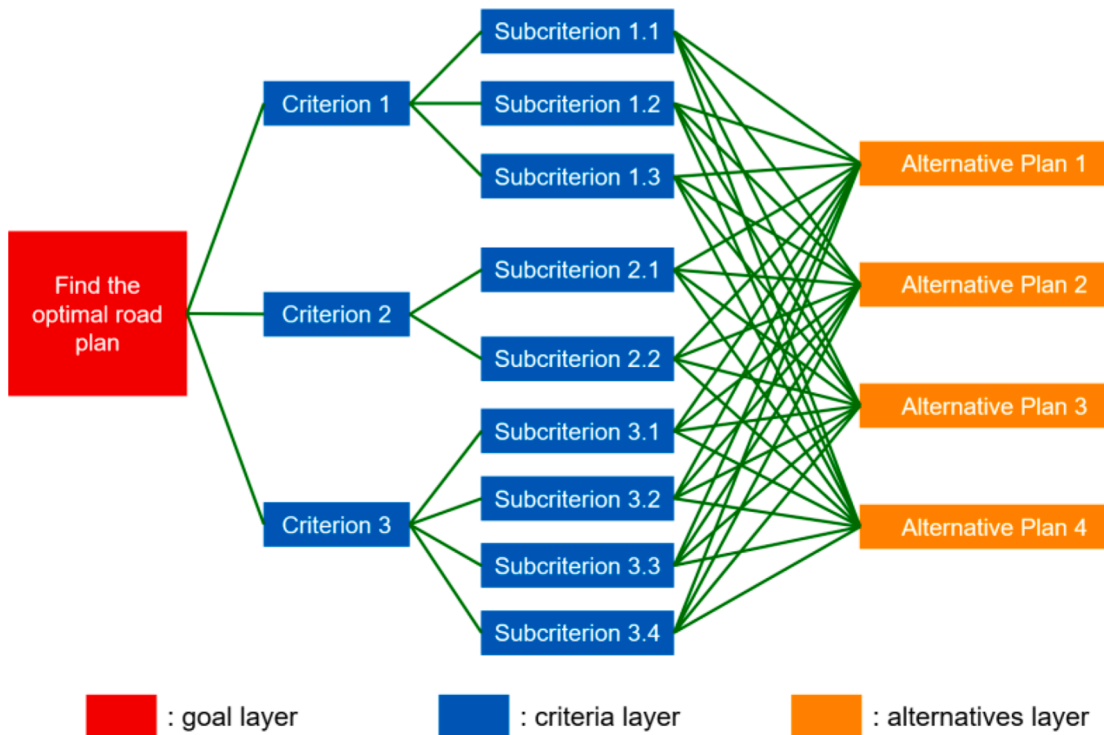


Fig. 1. The traditional structure of AHP for road planning.

2.3. Digital twin and related applications

A digital twin consists of five parts: physical part, virtual part, connection, data, and service. The physical part is the basis of the virtual part; the virtual part mirrors the physical part in a controlled setup; the connections enable data transfer and control (Tao, Zhang, Liu, & Nee, 2019). DT can be established to provide digital replicas for the environment, surroundings, and related existing projects according to point clouds, sensor data, design documents and other sources to assist planning and design (Jiang et al., 2021; O'Dwyer, Pan, Charlesworth, Butler, & Shah, 2020). Schrotter and Hürzeler (2020) took advantage of the digital twin to assist in the decision-making and city planning of the City of Zurich. Three-dimensional spatial data and their model transform urban entities (such as buildings, bridges, vegetation, etc.) into a digital world and update them when necessary to create advantages in digital space. White, Zink, Codéca, and Clarke (2021) presented a public and open digital twin of the Docklands area in Dublin, Ireland, which could assist in urban planning of skylines and green space and allow users to interact and report feedback on planned changes. Badawi, Laamarti, and Saddik (2021) designed a digital twin model of urban services to reflect the actual state of urban service development to improve citizens' quality of life. Marcucci, Gatta, Pira, Hansson, and Bråthen (2020) employed digital Twin to assist urban freight transport policy-making and planning. Schislyaeva and Kovalenko (2021) analysed digital twins in infrastructure and urban planning at various scales, from the characteristics of the simplest digital twin to the most complex part of the digital twin that could simulate the entire logistics terminal and the city to assist logistics networks routine operation. In the above studies, digital twins could improve the quality and accuracy of design significantly through data integration and high-fidelity models,

2.4. The gaps from the literature review

By considering various factors, sustainable urban road planning strives to meet current and future traffic-related demands and achieve financial, environmental, and social goals. However, according to the

literature review, some gaps still exist as follows:

- 1) Digital twin has not been widely used for road planning. Though some existing research proposed hybrid MCDM-GIS methods, they have not proposed a systematic approach to interpreting various data from the physical world into appropriate digital expressions to assist the MCDM process.
- 2) There are many existing buildings in a city, and the demolition of existing buildings is a critical constraint for urban road planning. However, no study considered the influence of building demolition costs considering various heights, sizes, and prices of different buildings for urban road planning.
- 3) From the perspective of being people-friendly, no study considered people's driving route selection habits for urban road planning.
- 4) In addition to newly built roads, many existing old roads in the city need to be upgraded. However, most of the road planning approaches focused on new road construction. They did not focus on new road construction and old road widening.

Thus, this paper proposes a novel DT-MCDM-GIS framework to interpret various data to assist urban road planning considering various sustainable factors, including building demolition and land use, traffic congestion, driving route selection habits, air quality, and noise. In addition, the proposed approach considers new road construction and existing old road widening. The following sections will introduce the proposed approach in detail.

3. An approach for sustainable urban road planning

The proposed approach focuses on the sustainable urban road planning for both new road construction and existing road widening considering the constraints from building demolition and land used, air quality, and noise to alleviate traffic congestion and provide an alternative route for drivers from a start point to an endpoint that conforms to the driving route selection habits. Urban road planning needs to balance the economic, social, and environmental constraints and the

Table 1
Random index.

n	1	2	3	4	5	6	7	8	9	10
RI	0.00	0.00	0.58	0.90	1.12	1.24	1.32	1.41	1.45	1.49

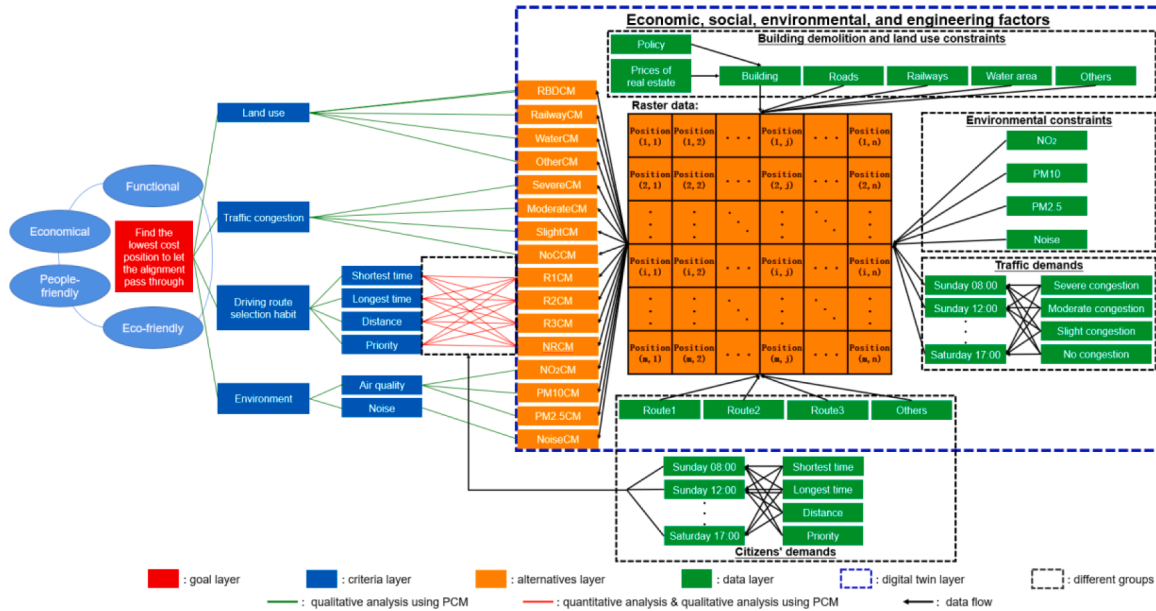


Fig. 2. The overall workflow for sustainable urban road planning based on the DT-MCDM-GIS framework.

functional demands from citizens to provide functional, economic, people-friendly, eco-friendly road planning schemes.

3.1. DT-MCDM-GIS framework for sustainable urban road planning

The traditional structure of AHP can be shown in Fig. 1. The weights of criteria can be estimated by the pairwise comparison matrix (PCM), as shown in Eqs. (1), where $0 < i, j \leq n$. $a_{ij}=3,5,7,9$ denote that criterion (i) is moderately more critical, strongly more important, very strongly more important, and extremely more important than criterion (j), respectively. $2,4,6,8$ are the intermediate values. $a_{ij}=1$ denotes that criterion (i) and criterion (j) are equally important. After the PCM is determined, the maximum eigenvalue (λ_{max}) of A and its corresponding eigenvector ω should be calculated, as shown in Eqs. (2). Afterwards, the consistency of the PCM should be checked according to Eqs. (3) and Eqs. (4), where n denotes that A is an $n \times n$ matrix, CI is the consistency index, CR is the consistency ratio, and RI is the random index, as shown in Table 1. The elements of the eigenvector ω can be described by Eqs. (5) and the weight of the criterion (i) can be described by Eqs. (6) (Saaty, 1990).

$$A = \begin{bmatrix} a_{11} & \cdots & a_{1n} \\ \vdots & \ddots & \vdots \\ a_{n1} & \cdots & a_{nn} \end{bmatrix}, a_{ii} = 1, a_{ji} = \frac{1}{a_{ij}}, a_{ij} \neq 0, a_{ij} = \frac{1}{2}, \frac{1}{3}, \dots, \frac{1}{9}, \text{ or } 1, 2, \dots, 9 \quad (1)$$

(1)

(2)

$$CI = \frac{\lambda_{max} - n}{n - 1} \quad (3)$$

(3)

$$CR = \frac{CI}{RI} \quad (4)$$

(4)

$$\omega = \begin{bmatrix} \omega_1 \\ \vdots \\ \omega_i \\ \vdots \\ \omega_n \end{bmatrix} \quad (5)$$

$$W(i) = \frac{\omega_i}{\sum_{i=1}^n \omega_i} \quad (6)$$

Generally, when using a PCM to evaluate the weights of alternatives, the alternatives in the same category in the same layer should preferably not be too many. Otherwise, it is too difficult to compare too many alternatives using a_{ij} . Thus, AHP was modified and combined with DT and GIS to form the overall workflow, as shown in Fig. 2. This research aims to find the lowest cost position in the goal layer to let the alignment pass through rather than finding the optimal road plan. In the criteria layer, various criteria are considered. In the digital twin layers, there are alternative layers and data layers. In the alternative layer, there is an $m \times n$ raster representing the target area, and each raster cell is an alternative. However, too many cells are evaluated directly by a PCM. Thus, various data are given to the raster cells to build various cost maps using DT. A cost map is a raster data, and each cell can be described by (i, j, C) , where i, j denote its position and C denotes the cost of the cell. However, C is not an actual cost with a unit but a value ranging from 0 to 255 (including 0 and 255). The lower the C is, the more the road alignment wants to go through the cell. In Fig. 2, RBDCM, RailwayCM, WaterCM, etc., various cost maps will be introduced in the following sections.

Generally, the weights for various criteria are determined by PCMs, usually established by experts or individuals by qualitative analysis, such as the PCM for building demolition and land use, traffic congestion, driving route selection habits, air quality, and noise. However, under the shortest time, most prolonged time, distance, and priority criteria, weighted average values should be calculated according to different specific values of the shortest time, most prolonged time, distance, and priority of a recommended route at different times. Then the weighted

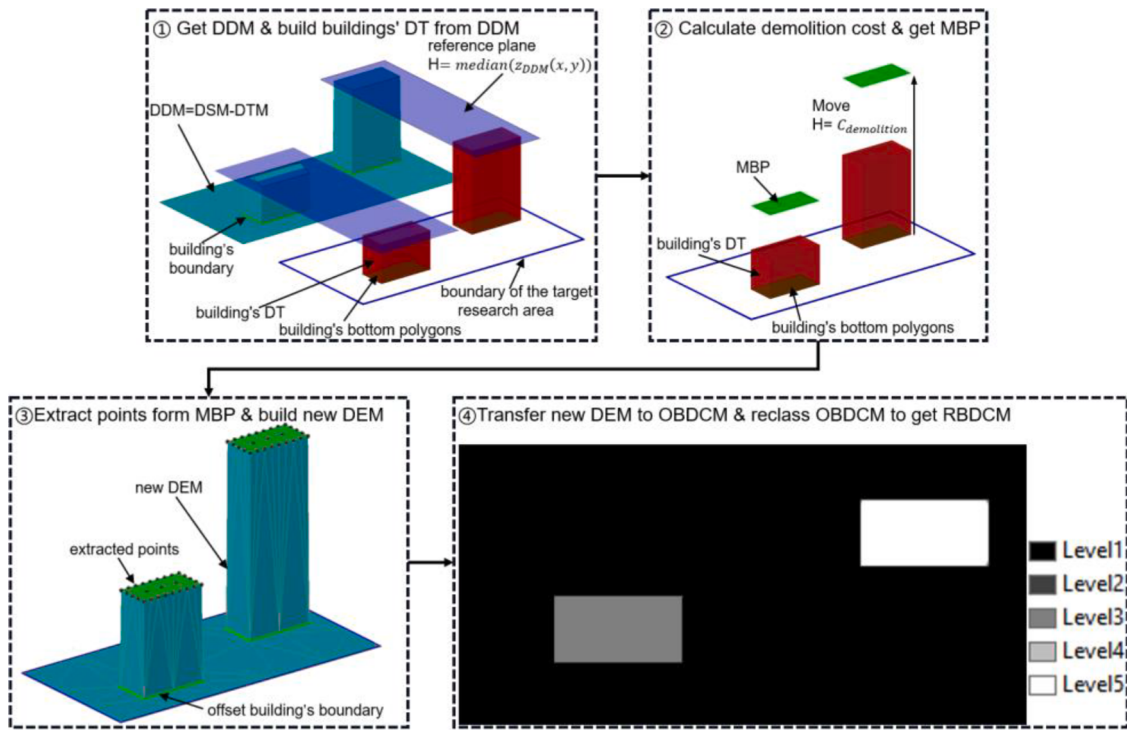


Fig. 3. Establish reclassified building demolition cost map (RBDCM) using DT and AHP.

average values are given to various recommended routes to determine the PCMs by quantitative analysis and qualitative analysis rather than determining the PCM directly by experts and individuals using qualitative analysis, which will be introduced in Section 3.4. Next, various cost maps are established and merged according to various PCMs to establish the overall cost map (Section 3.6). Then the road planning is conducted according to the OverallCM.

3.2. Building demolition and land use

To determine the building's land-use cost map, topographic maps, Digital Terrain Model (DTM) and Digital Surface Model (DSM) data are obtained through various map databases, such as Digimap (EDINA, 2021), Google Maps, Google Earth, OpenStreetMap, ArcGIS, etc. Points on DTM and DSM can be described by coordinates (x, y, z) , where x, y denotes the coordinate on the west-east horizontal axis, coordinate on the south-north horizontal axis, and the height of the point from the horizontal plane, respectively. For every two points with the same (x, y)

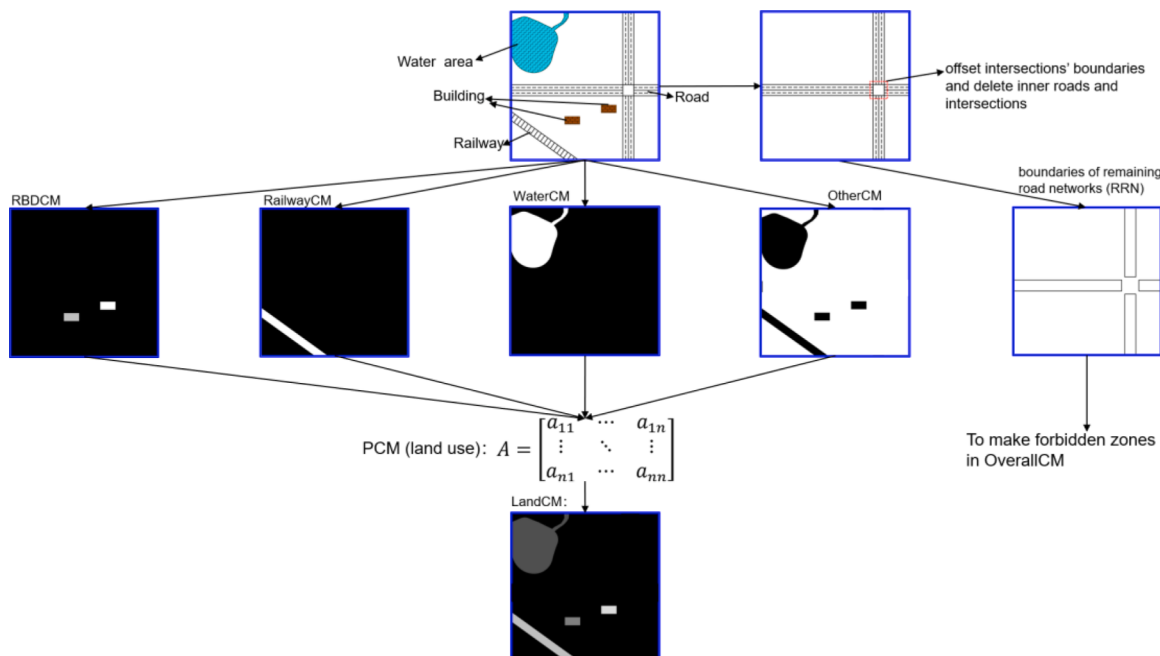


Fig. 4. Establish the overall land-use cost map (LandCM) using DT and AHP.

coordinate on DSM and DTM, the difference between the two points' z values can be calculated. Points with the coordinate (x,y,d) where d is the difference of z values at (x,y) can form a new digital elevation model called Digital Difference Model (DDM), as shown in Eqs. (7). In addition, the buildings' boundaries can be obtained from topographic maps, and they can form polygons that can be regarded as the bottom of the corresponding buildings called the building's bottom polygons. In the area inside a building's boundary and on the boundary, z values can be obtained from DDM, and Eqs can calculate the median value of these z values. (8), which can be regarded as the height of the building (H). The building's bottom polygons can be extruded along the positive direction of the z-axis by H to form simple digital twins for all buildings (① in Fig. 3). Afterwards, the demolition cost of the building can be calculated by Eqs. (9), where h is the average height from floor to floor of a building, V is the volume of a building's digital twin, S_{bottom} is the area of the building's bottom polygon, p is the average price of the building per square meter, μ is the amplification coefficient, and H is the same as the H in Eqs. (8). After that, the building's bottom polygons are moved along the positive direction of the z-axis by $C_{demolition}$ to form MBPs (Moved Building's Polygon) (② in Fig. 3). The points on the MBP can be extracted. Simultaneously, the buildings' boundaries polylines are offset by a minimal value outwards to ensure the projections of all the extracted points of MBP on the x-y plane are enclosed by the offset polylines. Then a new digital elevation model (DEM) can be established by the extracted points and the offset polylines, and the DEM can be transferred into raster data called the original building demolition cost map (OBDCM) (③ in Fig. 3). $C_{demolition}$ of buildings can be divided into several levels and levels' weights can be determined by PCM (RBDCM). All the positions (cells of the raster) can be given values from 0 to 255, and a new raster called reclassified building demolition cost map (RBDCM) can be established with their new values (④ in Fig. 3). The values of each cell of RBDCM (raster data) in Level i can be calculated by Eqs. (10), where ω_i denotes the value in Eqs. (5) of the PCM (RBDCM).

$$z_{DDM}(x, y) = z_{DSM}(x, y) - z_{DTM}(x, y) \quad (7)$$

$$H = \text{median}(z_{DDM}(x, y)), (x, y) \in \text{Area}_{on \text{ and } within \text{ the boundary}} \quad (8)$$

$$C_{demolition} = \mu \frac{V}{h S_{bottom}} \cdot p \cdot S_{bottom} = \mu \frac{V \cdot p}{h} = \mu \frac{H}{h} \cdot S_{bottom} \quad (9)$$

$$V_{RBDCM}(i) = 255 \frac{\omega_i - \min(\omega_i)}{\max(\omega_i) - \min(\omega_i)} \quad (10)$$

In addition to the building demolition cost map, existing roads are a significant factor for road planning. In the existing road areas, forbidden zones should be set on the OverallCM. Forbidden zones are the areas with no data on OverallCM, and they are not involved in analysis and calculations. Thus, the new road alignment will not occupy the existing road. However, if the intersection areas are set as forbidden zones, it may hinder the generated alignment from going through intersections. Thus, polygons are employed to describe the road networks, and the boundaries of intersections are extracted and offset an appropriate value outwards. Then, inside the offset boundaries, the polygons of roads and intersections are cut and deleted. The boundaries of the remaining road networks (RRN) can be extracted, and in the RRN's areas, forbidden zones should be set, as shown in Fig. 4.

In addition to the RBDCM, other cost maps only consider a single factor should be established. First, existing railways and water areas should be determined by topographic maps or digital image processing from maps or satellite maps and expressed by polylines or polygons. Then, new raster maps describing various land-use cost maps should be established by the polylines or polygons. For a railway land-use cost map (RailwayCM), the raster's values of the positions in the areas of existing railways are set to 255, and values in other positions are set to 0. It is similar to the water area cost map (WaterCM). Besides, a new raster called other land-use cost map (OtherCM) is established. The raster

values are set to 0 if the position is in the existing buildings, railways, or water areas. In other areas, the values are set to 255.

After cost maps are determined, a PCM (land use) is established to determine their weights. The overall land-use cost map (LandCM) can be established using RBDCM, RailwayCM, WaterCM, OtherCM and their weights, as shown in Fig. 4. All the cost maps are $m \times n$ raster data in the same size, and the value of each cell can be expressed by $Cell_{i,j}$, where $1 \leq i \leq m$, $1 \leq j \leq n$ and i, j are integers. Eqs can calculate the value of each cell of LandCM. (11), where Y denotes the LandCM, X denotes RBDCM, RailwayCM, WaterCM, or OtherCM, and $W(X)$ denotes their weights from PCM.

$$Cell_{i,j}(Y) = \sum Cell_{i,j}(X) \cdot W(X) \quad (11)$$

3.3. Traffic congestion

Traffic congestion situations at various times in the target research area can be obtained from Google Maps. Screenshots of the same size can save traffic congestion situations. In this research, typical traffic congestion in the target research area at various times from Sunday to Saturday can be captured by screenshots of the same size ($u \times v$ pixels). In these images from screenshots, the positions of the existing roads coloured in red, orange, and green mean that the position has severe traffic congestion, moderate traffic congestion, and smooth traffic, respectively. Colours on these images can be controlled by R, G, B (red, green, blue) values, and R, G, B values are 0–255 integers. Since only red, orange, yellow, green represent the severity of traffic congestion, and orange and yellow can be obtained by combining red and green, the severity of the traffic congestion can be controlled only by R and G values. The greener positions mean that their traffic is less congested, and the redder positions mean that their traffic is more congested. Thus, G/R is employed to represent the severity of traffic congestion. In addition, the blue values of the colours representing traffic congestion are very low, and the blue values of the colours in the remaining areas are generally relatively high. Thus, a threshold (B_T) is given to the B values of the colours to get the areas representing the traffic congestion and filter the remaining areas. Hence, R, G, B values can be employed to analyze the images.

Afterwards, appropriate weights should be given to the screenshots to form an overall traffic congestion map. The more serious the traffic congestion is at a time, the higher weight will be given to the time for road planning. By digital image processing, (R,G,B) values of all the images are covered to (r,g,b) values, where r, g, b are the numbers with 0–1 double-precision decimals. The relationships between (R,G,B) and (r,g,b) can be expressed by Eqs. (12). Similarly, a threshold called b_T can be calculated by $B_T/255$. For each image, the number of pixels whose $g/r \leq 0.4$ and $b \leq b_T$ is represented by n_{red} and the number of pixels whose $g/r > 0.4$ and ≤ 0.8 , and $b \leq b_T$ is represented by n_{orange} . There are n captured images representing the traffic congestion and the traffic congestion index of Image k ($TC(k)$) can be calculated by Eqs. (13). The weight given to Image k ($W(k)$) can be calculated by Eqs. (14). After that, a new image called Image F can be obtained by fusing all the images from screenshots according to their weights. All the images from screenshots and Image F have the same size ($u \times v$ pixels). r,g,b values of each pixel in Image F can be calculated by Eqs. (15), where a, b denote the position of a pixel in Image F, $1 \leq a \leq u$, $1 \leq b \leq v$, and a, b are positive integers. $r(k)_{a,b}$, $g(k)_{a,b}$, $b(k)_{a,b}$ denote the r, g, b values of the pixel at the position of (a,b) in Image k.

$$r = \frac{R}{255}; g = \frac{G}{255}; b = \frac{B}{255} \quad (12)$$

$$TC(k) = n_{red} + 0.5n_{orange} \quad (13)$$

$$W(k) = \frac{TC(k)}{\sum_{i=1}^n TC(k)} \quad (14)$$

Table 2
Standardize the image F to image S.

Conditions of Image F	r,g,b of Image F	r,g,b of image s	color	Traffic congestion
$0 \leq g/r \leq 0.4$ $\& b \leq b_T$	r g b	1 0 0	Red	Severe
$0.4 < g/r \leq 0.8$ $\& b \leq b_T$	r g b	1 0.5 0	Orange	Moderate
$0.8 < g/r \leq 1.2$ $\& b \leq b_T$	r g b	1 1 0	Yellow	Slight
$1.2 < g/r$ $\& b \leq b_T$	r g b	0 1 0	Green	No

$$r(F) = \sum_{k=1}^n r(k)_{a,b} W(k), \quad g(F) = \sum_{k=1}^n g(k)_{a,b} W(k), \quad b(F) = \sum_{k=1}^n b(k)_{a,b} W(k) \quad (15)$$

The colours represent traffic congestion transition from red to green in the existing road areas. Thus, it is tough to determine which position is red, orange, yellow or green and where traffic congestion is severe, moderate, slight, or there is no traffic congestion. Thus, Image F needs to be standardized to make a new image called Image S. The conversion method can be expressed by Table 2, where r,g,b values of Image F are replaced by appropriate values to obtain the r,g,b values of Image S. The process can be shown in Fig. 5.

After that, Image S can be aligned with the edges of remaining road networks (RRN) without intersections, as shown in Image ① in Fig. 6. If the traffic congestion is severe in a section of an existing road, it is better to widen the existing road to alleviate the traffic congestion. The edges of RRN where Image S is red, orange, and yellow are offset outwards to make offset areas with the original edges. The offset areas can be divided into severe, moderate, and slight traffic congestion separately. The traffic congestion denotes the traffic congestion of the lanes of original existing roads with the same driving direction excluding the opposite

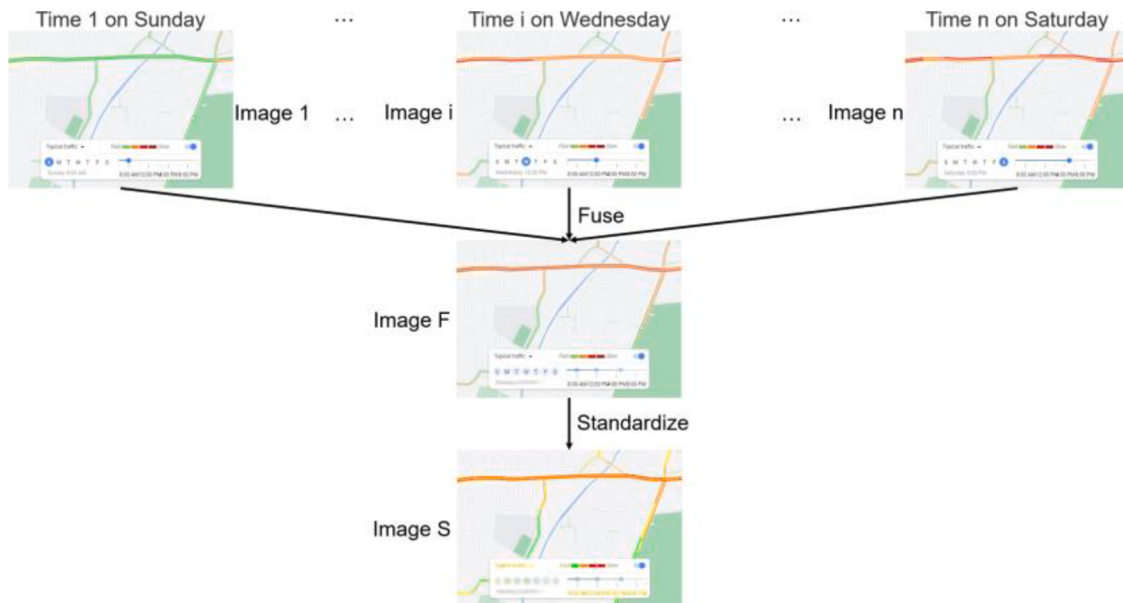


Fig. 5. Digital image processing for traffic congestion.

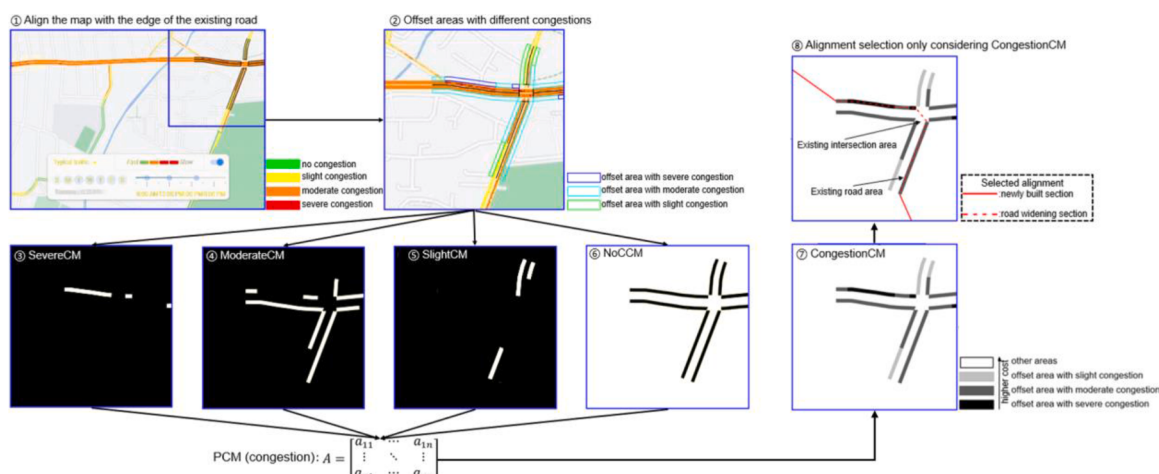


Fig. 6. Establish a traffic congestion cost map (CongestionCM).



Fig. 7. Calculate weighted average driving time, distance, priority of each route according to traffic congestion.

lanes, and adjacent to the offset areas, as shown in Image ② in Fig. 6. Thus, there is an offset area on each side of the road according to the driving direction of the adjacent lane. Afterwards, cost maps only considering offset areas with severe, moderate, or slight traffic congestion are established, which are called severely congested cost map (SevereCM) (③ in Fig. 6), moderately congested cost map (ModerateCM) (④ in Fig. 6), and slightly congested cost map (SlightCM) (⑤ in Fig. 6), respectively. In SevereCM, ModerateCM and SlightCM, in the corresponding offset areas, the values are set to 255, and in other areas, the values are set to 0. Additionally, a cost map called no congestion cost map (NoCCM) is established where the values are set to 0 in all offset areas, and values are set to 255 in other areas (⑥ in Fig. 6). Then, an appropriate PCM (congestion) is made for SevereCM, ModerateCM, SlightCM, and NoCCM to establish an overall traffic congestion cost map (CongestionCM) (⑦ in Fig. 6). Similarly, the value of each cell of the CongestionCM can be calculated by Eqs. (11). To ensure the generated

alignment has the trend to go through the areas with severer traffic congestion, SevereCM needs to be given the minimum weight, and NoCCM needs to be given the maximum weight.

3.4. Driving route selection habit

This study assumes that people always prefer to drive from the start to the endpoint via recommended routes from Google Maps or other satellite navigation platforms. Thus, it is better to widen the recommended routes. To realize road planning considering driving route selection habits, recommended routes from the start point to the endpoint can be queried from Google Maps at various times from Sunday to Saturday (Time 1, ... Time k, ... Time n). Similarly, corresponding weights $W(k)$ according to the traffic congestion at various times in Eqs. (14) are given to various times. Four factors of the recommended routes at various times are considered: shortest time (ST(k, r)), longest time (LT

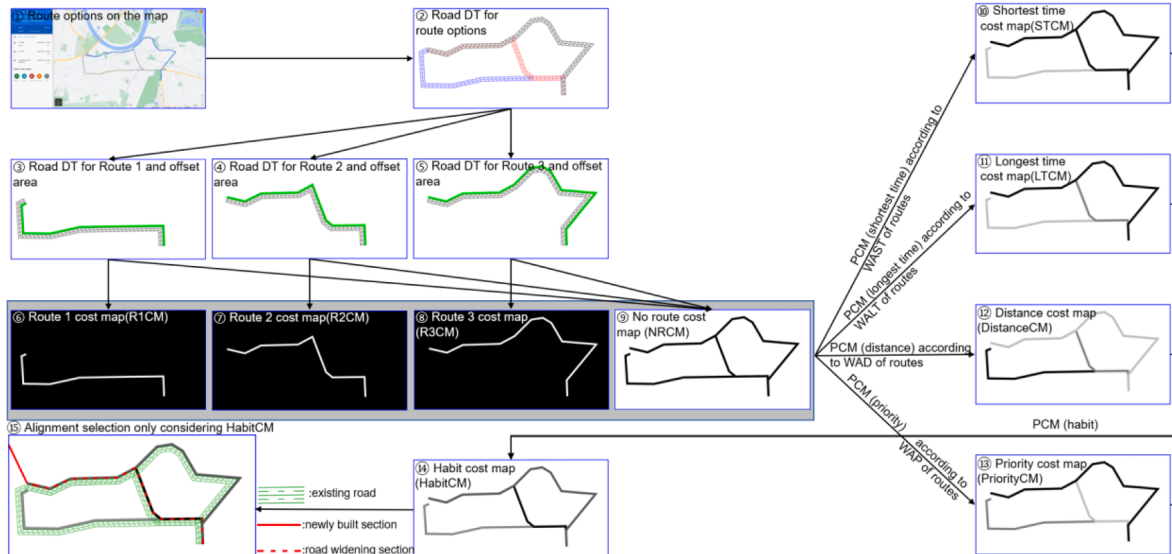


Fig. 8. Establish driving route selection habit cost map (HabitCM).

(k, r)), distance $D(k, r)$), and priority $P(k, r)$ which denote the estimated typical shortest driving time via a recommended route (Route r) at Time k , the estimated typical longest driving time via a recommended route (Route r) at Time k , and the length from the start point to the end point via a recommended route (Route r) at Time k , and the recommendation priority of a recommended route (Route r) among all recommended routes at Time k , respectively. For the priority, the value of the first recommended route is set to 1; the value of the second recommended route is set to 2; and so on. The weighted average values of these four factors at various times can be calculated by Eqs. (16)-(19), where WAST(r), WALT(r), WAD(r), WAP(r) denote the weighted average shortest time, longest time, distance, and priority of Route r , respectively. The process can be shown in Fig. 7. Afterwards, weighted average values of factors need to be normalized by Eqs. (20)-(23).

$$WAST(r) = \sum_{k=1}^n ST(k, r)W(k) \quad (16)$$

$$WALT(r) = \sum_{k=1}^n LT(k, r)W(k) \quad (17)$$

$$WAD(r) = \sum_{k=1}^n D(k, r)W(k) = D(k, r) \quad (18)$$

$$WAP(r) = \sum_{k=1}^n P(k, r)W(k) \quad (19)$$

$$WAST_{\text{normalize}}(r) = \frac{WAST(r) - \min(ST(k, r))}{\max(ST(k, r)) - \min(ST(k, r))} \quad (20)$$

$$WALT_{\text{normalize}}(r) = \frac{WALT(r) - \min(LT(k, r))}{\max(LT(k, r)) - \min(LT(k, r))} \quad (21)$$

$$WAD_{\text{normalize}}(r) = \frac{WAD(r) - \min(D(k, r))}{\max(D(k, r)) - \min(D(k, r))} \quad (22)$$

$$WAP_{\text{normalize}}(r) = \frac{WAP(r) - \min(P(k, r))}{\max(P(k, r)) - \min(P(k, r))} \quad (23)$$

After that, the digital twin of the roads from the selected routes can be simply established (② in Fig. 8), and the intersections boundaries are offset outwards and employed to delete the roads and intersections inside. Similar to Section 3.3, the boundaries of the remaining roads can be extracted and offset outwards by a suitable value to form offset areas. Unlike Section 3.3, the offset area in this section is only on one side of the road. If the local traffic rules require driving on the left, the offset area is only established on the left side of the target roads and vice versa (③, ④, ⑥ in Fig. 8). Then the cost maps called Route r cost map (RrCM) only considering the offset areas of a single recommended route (Route r) are established, where the values are set to 255 in the offset areas of a single recommended route, and the values are set to 0 in the remaining areas (⑥, ⑦, ⑧ in Fig. 8). In addition, a cost map called no route cost map (NRCM) (⑨ in Fig. 8) is established where the values are set to 0 in the offset areas of all recommended routes, and the values are set to 255 in the remaining areas. Afterwards, appropriate PCM (ST), PCM (LT), PCM (distance), PCM (priority) are established by qualitative and quantitative analysis to evaluate all the recommended routes under the four factors, respectively, to give weights to RrCMs and NRCM to establish shortest time cost map (STCM), longest time cost map (LTCM), distance cost map (DistanceCM), and priority cost map (PriorityCM), by Eqs. (11), (10), (11), (12), (13) in Fig. 8. For road planning, the smaller the values of $WAST_{\text{normalize}}(r)$, $WALT_{\text{normalize}}(r)$, $WAD_{\text{normalize}}(r)$, $WAP_{\text{normalize}}(r)$ of the corresponding recommended routes (Route r) are, the lower cost values are given to their offset areas. In addition, NRCM should have a significantly higher score in PCMs than RrCM. According to Eqs. (1), in PCMs for STCM, LTCM, DistanceCM, and PriorityCM, a_{ij}

Table 3

Determine the elements of PCMs by qualitative and quantitative analysis.

Object to compare	Element	Range	Values of a_{ij} or a_{in}
RiCM and RjCM	a_{ij}	$0 \leq WAX_{\text{normalize}}(i) - WAX_{\text{normalize}}(j) \leq 0.01$	1
		$0.01 < WAX_{\text{normalize}}(i) - WAX_{\text{normalize}}(j) \leq 0.25$	2
		$0.25 < WAX_{\text{normalize}}(i) - WAX_{\text{normalize}}(j) \leq 0.5$	3
		$0.5 < WAX_{\text{normalize}}(i) - WAX_{\text{normalize}}(j) \leq 0.75$	4
		$0.75 < WAX_{\text{normalize}}(i) - WAX_{\text{normalize}}(j) \leq 1$	5
		$-0.01 \leq WAX_{\text{normalize}}(i) - WAX_{\text{normalize}}(j) \leq 0$	1
		$-0.25 \leq WAX_{\text{normalize}}(i) - WAX_{\text{normalize}}(j) < 0.01$	1/2
		$-0.5 \leq WAX_{\text{normalize}}(i) - WAX_{\text{normalize}}(j) < -0.25$	1/3
		$-0.75 \leq WAX_{\text{normalize}}(i) - WAX_{\text{normalize}}(j) < -0.5$	1/4
		$-1 \leq WAX_{\text{normalize}}(i) - WAX_{\text{normalize}}(j) < -0.75$	1/5
RiCM and NRCM	a_{ni}	$0 \leq WAX_{\text{normalize}}(i) \leq 1/3$	9
		$1/3 < WAX_{\text{normalize}}(i) \leq 2/3$	8
		$2/3 < WAX_{\text{normalize}}(i) \leq 1$	7

denotes the comparison between Route i cost map (RiCM) and Route j cost map (RjCM). a_{in} or a_{jn} denote the comparison between Route i cost map (RiCM) or Route j cost map (RjCM) and no route cost map (NRCM). If there are $n-1$ recommended routes from Google Maps, $WAX_{\text{normalize}}(i)$ of Route i denotes the $WAST_{\text{normalize}}(i)$, $WALT_{\text{normalize}}(i)$, $WAD_{\text{normalize}}(i)$, or $WAP_{\text{normalize}}(i)$, where i is an integer and $1 \leq i \leq n-1$. The elements of PCMs can be determined according to $WAX_{\text{normalize}}(i)$ as shown in Table 3. After STCM, LTCM, DistanceCM, PriotyCM are established, an appropriate PCM (habit) is established to give appropriate weights to them to establish the driving route selection habit cost map (HabitCM) (⑩ in Fig. 8).

3.5. Environment

This research considers three air pollutants (NO_2 , PM10 , PM2.5) and noise. There are two main reasons to consider these criteria. First, in a city, vehicles contribute a lot of air pollutants and noise. The higher concentration of air pollutants and louder noise means more economic activities and more vehicles. Thus, road network expansion needs to be conducted in these areas. Second, road construction also can produce more air pollutants and noise. Thus, road construction is preferably conducted in the areas with denser pollutants and louder noise to avoid disturbing the residents in other quiet areas with better air quality. A workflow is proposed to make cost maps for air pollutants and noises distribution, as shown in Fig. 10 Reference source not found.

First, screenshots of the online air pollutant maps and noise maps can be captured from the web page and are aligned with the correct coordinates of the target research area by moving, rotating, and scaling, as shown in ① in Fig. 10 Reference source not found. The aligned screenshot can be regarded as a three bands (r,g,b) raster and each Cell (i,j) of the raster has a specific Color (i,j) which can be described by $(r(i, j), g(i, j), b(i, j))$.

Second, according to the legend, different colours denote different densities of the air pollutants or different decibel values of the noises. There are several colours in the legend called standard colours. Some of these colours are used in screenshots, and each used color can be described by Color (x) , where $1 \leq x \leq n$. color (x) can be expressed by a three-dimensional coordinate $(r(x), g(x), b(x))$. Correspondingly, there

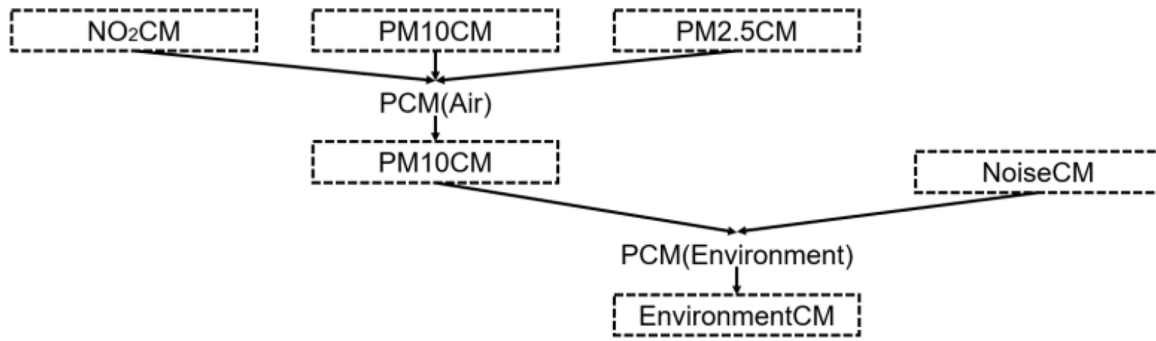
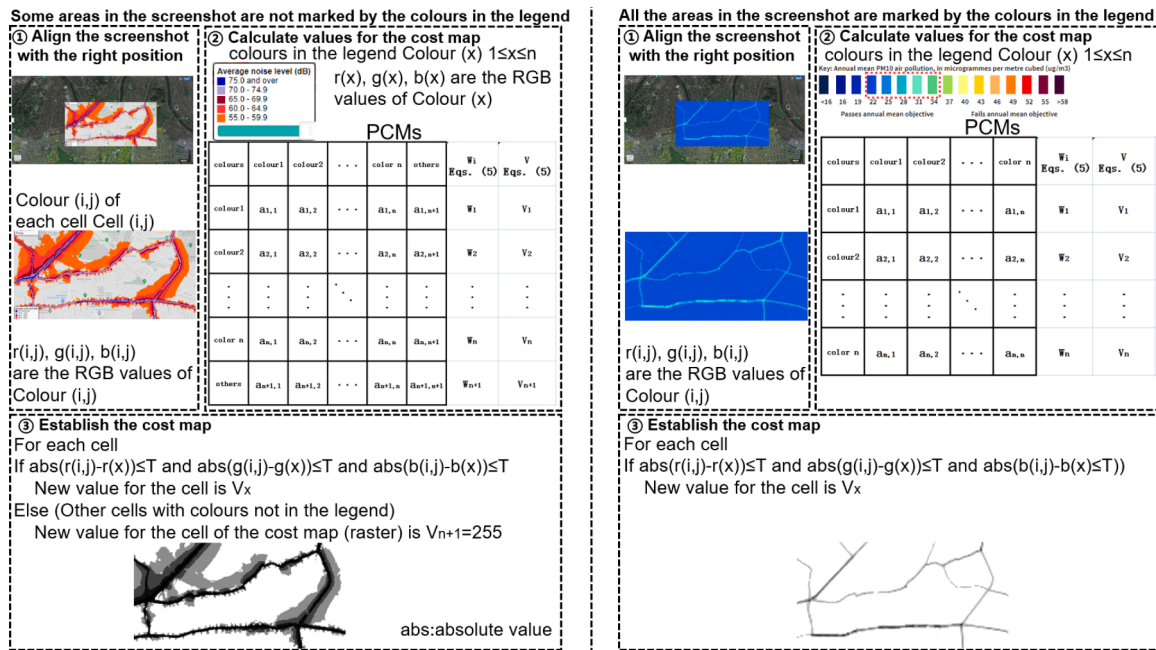


Fig. 9. Make cost maps for air pollutants and the environment.

Fig. 10. Make cost maps for NO₂, PM10, PM2.5, and noise.

are n levels representing different densities of the air pollutants or different decibel values of the noises marked in different standard colours that can be represented by Level x . In addition to Level x , Level $n + 1$ represents the other areas that are not marked in standard colours, where there are the sparsest air pollutants or lowest noises, as shown in the left process in Fig. 10. According to MCDM, appropriate PCMs (PCM (NO₂), PCM(PM10), PCM(PM2.5), PCM(noise)) are established for different screenshots to give weights to the levels, and new values are given to different levels according to Eqs. (24), where ω_i is the eigenvector's elements for Level x according to PCM (Eqs. (5)), V_x is the value given to Level x , ω_{n+1} is the eigenvector's elements for of Level $n + 1$, and V_{n+1} is the value given to Level $n + 1$, as shown in ② in Fig. 10. Some screenshots do not have Level $n + 1$, which means all the screenshots are marked in standard colours in the legend, as shown in the right process in Fig. 10. The level representing higher pollutant concentration and louder noise needs to be given a lower weight by PCM and value V_x . Thus, the planned road has the trend to go through the areas with higher pollutant concentration and louder noise.

Third, there may be slight deviations between the colours in the screenshots and the standard colours in the legend. Thus, Color (i,j) of each cell (i,j) of the screenshot should be compared with Color (x). If the absolute values of $r(i,j)-r(x)$, $g(i,j)-g(x)$, and $b(i,j)-b(x)$ are all no greater than the tolerance (T), V_x is given to the cell as the raster value. If the $r(i,j)$, $g(i,j)$, $b(i,j)$ cannot meet the tolerance compared to $r(x)$, $g(x)$, $b(x)$ of

all used color in the legend, V_{n+1} is given to the cell. All cells Cell (i,j) and their given values can establish the cost map for NO₂, PM10, PM2.5, and noise, called NO₂CM, PM10CM, PM2.5CM, and NoiseCM, as shown in ③ in Fig. 10.

Fourth, an appropriate PCM(Air) is established to give weights to NO₂CM, PM10CM, PM2.5CM to build the cost map for air quality (AirCM). Then an appropriate PCM (environment) is established to give weights to AirCMs and NoiseCM to build the cost map for the environment (EnvironmentCM), as shown in Fig. 9. The values of each cell of the AirCM and EnvironmentCM can be calculated by Eqs. (11).

$$V_x = 255 \frac{\omega_x}{\sum_{i=1}^{n+1} \omega_x}, V_{n+1} = 255 \frac{\omega_{n+1}}{\sum_{i=1}^{n+1} \omega_x}, \text{ or } V_x = 255 \frac{\omega_x}{\sum_{i=1}^n \omega_x} \quad (24)$$

3.6. Road planning

After LandCM, CongestionCM, HabitCM and EnvironmentCM are determined, appropriate weights are given to them by PCM (overall) to establish the overall cost map (OverallCM). In the OverallCM, remaining road networks (RRN) areas are set as forbidden zones. In addition, some areas are set as forbidden, such as essential landmarks, historical heritage, tombs, etc. In the forbidden zones, there are no data rather. Thus, forbidden zones are not involved in analysis and calculations, and the generated alignment cannot occupy the forbidden zones. Afterwards,

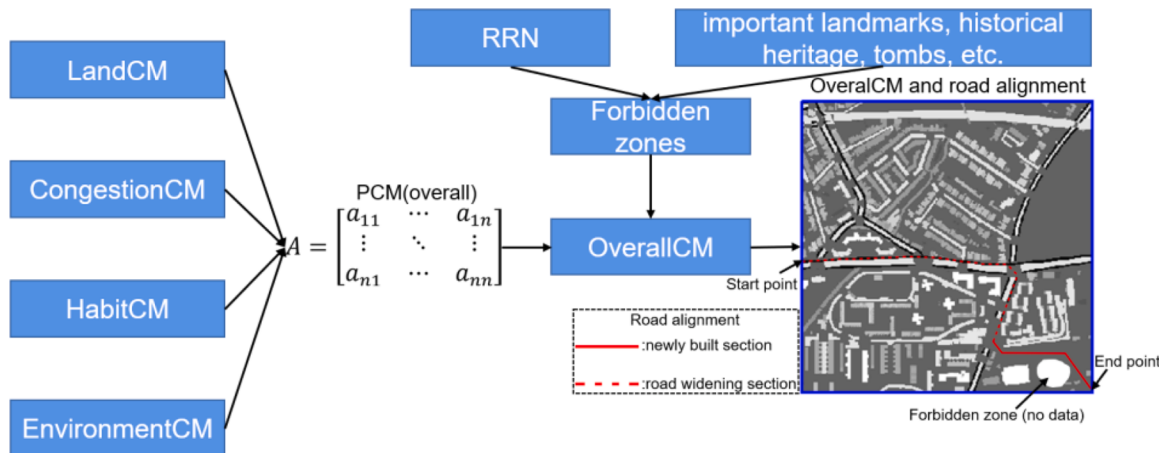


Fig. 11. Overall cost map (OverallCM) establishment and road planning.

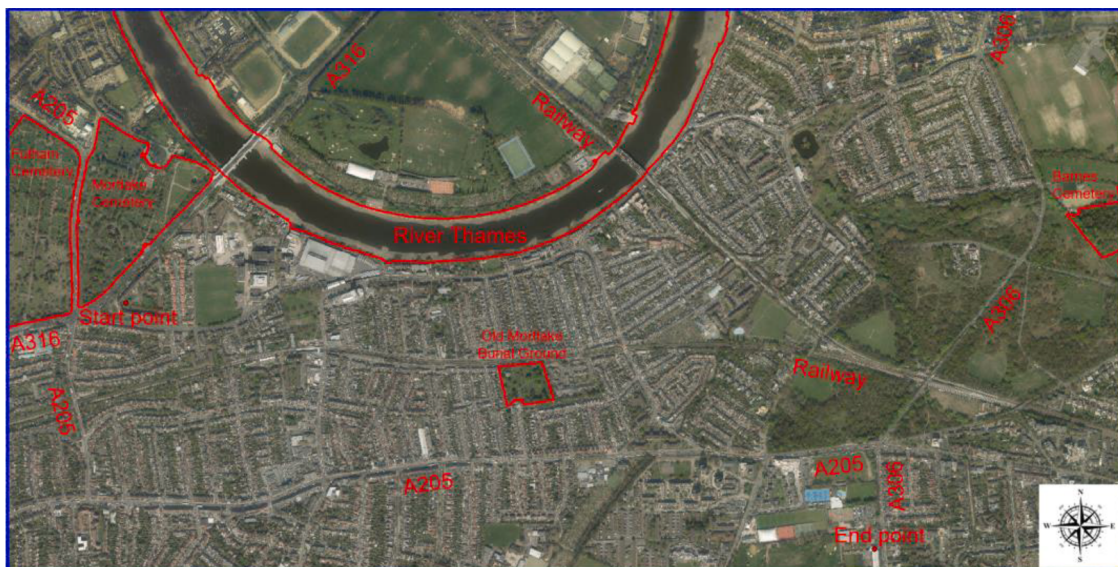


Fig. 12. The target research area.

ArcGIS establishes a start point and an endpoint, and a cost distance map and cost back link map are established based on the OverallCM. Then a cost path can be produced by ArcGIS, which can represent the result of the urban road planning, as shown in Fig. 11. The generated alignment tries to go through the darker areas on the OverallCM, avoiding the forbidden zones. If the alignment goes along the side of the road, it is a road-widening section. Other sections of the alignment are newly built sections.

4. Case study

The proposed approach was implemented in Mortlake in the southwest of London. DEM, DSM, topographic maps, aerial photograph data were downloaded from Digimap (EDINA, 2021). Traffic congestion data and recommended driving route data were downloaded from Google Maps. N0₂, PM10, PM2.5 data were downloaded from the future maps in 2020 from London Air (Imperial College London, 2021). Noise data were downloaded from England Noise and Air Quality Viewer made by Extrium in 2017, and data were day-evening-night data (Extrium, 2017). Cost Distance, Cost Back Link, and Cost Path functions of ArcGIS 10.3.1 were employed for road planning.

4.1. Introduction of the target research area

The latitude and longitude coordinates of the southwest corner and northwest corner of the target research area are 51°27'45.350039"N 0°16'47.212426"W and 51°28'34.688804"N 0°13'59.781527"W, as shown in Fig. 12. The target research area is relatively remote compared to the core area of London, where there are many low-rise residential buildings, commercial buildings, some low-rise public buildings, three high-grade roads (A316, A205, A306), some low-grade road networks, two crossed railway lines, some green areas and gardens, some water areas and small rivers, and a section of River Thames in the north. In addition, there are some cemeteries, and the cemeteries and the River Thames are set as forbidden zones. Therefore, traffic congestion in the target research area is relatively severe at peak times. In addition, although there are many buildings in this area, there are still some open spaces that allow the expansion and widening of the road network. The coordinates of the road planning's start point are 51°28'9.800870"N 0°16'28.733227"W, which is Chertsey Court. The court is located to the northeast of road A316 and road A205. It is an important point for vehicles entering and exiting the area from and to the outside. The coordinates of the endpoint are 51°27'45.458140"N 0°14'38.788432"W, which is called Thomas Dolphin. There are two colleges and a university in the endpoint's southern area. The planning has a significant and

Table 4

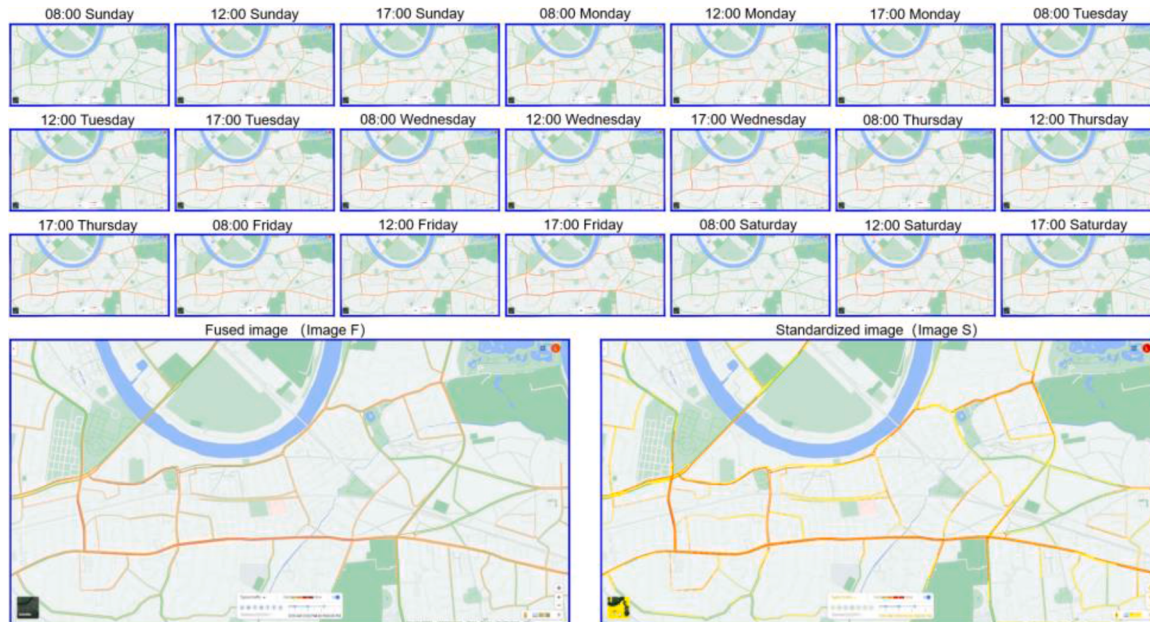
Reclassified building demolition cost map (RBDCM) and its PCM (RBDCM).

Levels	1	2	3	4	5	6	7	8	9	ω_i	OBDCM values	RBDCM values
1	1	1/9	1/9	1/9	1/9	1/9	1/9	1/9	1/9	0.0349	0–0.1	0
2	9	1	1/2	1/2	1/2	1/2	1/2	1/2	1/2	0.183	0.1–1.112	75
3	9	2	1	1/2	1/2	1/2	1/2	1/2	1/2	0.213	1.112–1.500	91
4	9	2	2	1	1/2	1/2	1/2	1/2	1/2	0.249	1.500–2.613	109
5	9	2	2	2	1	1/2	1/2	1/2	1/2	0.291	2.613–5.803	130
6	9	2	2	2	2	1	1/2	1/2	1/2	0.339	5.803–14.954	154
7	9	2	2	2	2	2	1	1/2	1/2	0.395	14.954–41.199	183
8	9	2	2	2	2	2	2	1	1/2	0.461	41.199–116.470	216
9	9	2	2	2	2	2	2	2	1	0.538	116.470–332.355	255
Values	λ_{max}		Consistency ratio									Consistency
Results	9.507		0.0437									Pass

Table 5

PCM (land use) for the land-use cost map (LandCM).

Cost map	RBDCM	RailwayCM	WaterCM	OtherCM	ω_i	$W(i)$
RBDCM	1	2	5	9	0.834	0.518
RailwayCM	1/2	1	3	9	0.509	0.316
WaterCM	1/5	1/3	1	5	0.206	0.128
OtherCM	1/9	1/9	1/5	1	0.0611	0.0380
Values	λ_{max}		Consistency ratio			Consistency
Results	4.115		0.0428			Pass

**Fig. 13.** Traffic congestion at various times from Google Maps, fused images, and standardized images.

positive effect on alleviating the pressure of the traffic flow from the outside area to the target research area via the intersection of road A316 and road A205.

4.2. Original data and specified parameters

DSM data and DTM data can be obtained from Digimap. Afterwards, the digital twin of buildings and the heights (H in Eqs. (8)), the areas of the bottoms (S_{bottom}), the volumes (V) of buildings' digital twins can be obtained. The target research area belongs to three zones: Hounslow, Richmond upon Thames, and Wandsworth, where the average house prices are 5969£, 8175£, 9661£ per square meter in 2016 according to the government's data (Office for National Statistics, 2017). Though there has been no official data of average house prices per square meter

in recent years, the monthly average total price of a house in the areas from 2016 to the recent month can be obtained (HM Land Registry Open Data, 2021). The monthly average total prices of a house of a zone from January to December in 2016 are summed and divided by 12 to represent the average total prices of a house in 2016. Then, 5969£, 8175£, 9661£ are multiplied by the average total prices of a house in February in 2021 and divided by the average total prices of a house in 2016, respectively, to represent the average house prices per meter in February 2021, which are 6657.657£, 8585.891£, 9795.568£ per square meter (p in Eqs. (9)). Generally, the average floor to floor height of a building is 3.2 m in London (Old Oak and Park Royal Development Corporation, 2018); thus, h is set to 3.2. In the UK, owner-occupiers who are eligible for compensation for house losses are entitled to 10% of the market value of the interest in the property. In addition, the owner of the

Table 6

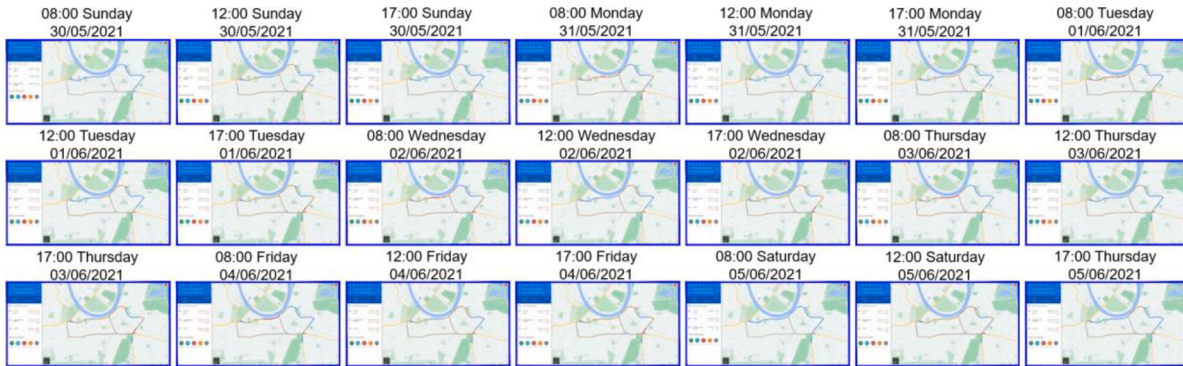
Weights of traffic congestion situations at various times.

Day	Time	Congestion index $TC(k)$	Weight $W(k)$	Day	Time	Congestion Index $TC(k)$	Weight $W(k)$
Sunday	8:00	4057.0	0.00865	Thursday	8:00	25,703.0	0.05482
	12:00	26,542.0	0.05661		12:00	21,321.5	0.04548
	17:00	16,093.5	0.03433		17:00	28,053.5	0.05984
Monday	8:00	22,921.5	0.04889	Friday	8:00	22,274.5	0.04751
	12:00	19,725.0	0.04207		12:00	24,702.0	0.05269
	17:00	22,684.5	0.04839		17:00	28,273.5	0.06031
Tuesday	8:00	27,133.5	0.05788	Saturday	8:00	5608.0	0.01196
	12:00	20,571.5	0.04388		12:00	30,272.5	0.06457
	17:00	26,761.0	0.05708		17:00	19,991.0	0.04264
Wednesday	8:00	28,052.0	0.05983				
	12:00	21,494.0	0.04585				
	17:00	26,592.5	0.05672				

Table 7

PCM (congestion) for the traffic congestion cost map (CongestionCM).

Cost map	SevereCM	ModerateCM	SlightCM	NoCCM	ω_i	$W(i)$
SevereCM	1	1/3	1/5	1/9	0.0593	0.0431
ModerateCM	3	1	1/3	1/8	0.116	0.0842
SlightCM	5	3	1	1/7	0.240	0.174
NoCCM	9	8	7	1	0.962	0.699
Values	λ_{max}		Consistency ratio		Consistency	
Results	4.262		0.0970		Pass	

**Fig. 14.** Recommended routes at various times from Google Maps.

building can claim other reasonable expenses related to the purchase or lease of another property (but not the property price or rent itself) and reasonable expenses of moving in and changing the new property (Department for Communities and Local Government, 2010). Thus, the μ can be set to 1.2 in this research. Then, Eqs. (9) is employed to determine the demolition cost of the target research area and establish OBDCM. After that, OBDCM is reclassified and divided into eight levels. The PCM (RBDCM) and the reclassification result can be shown in Table 4. The PCM (land use) and the weights given to different cost maps to establish the LandCM can be shown in Table 5.

Screenshots of the typical traffic congestion situations at various times from Google Maps are as shown in Fig. 13, and their congestion indexes ($TC(k)$) and weights ($W(k)$) can be calculated by Eqs. (13) and Eqs. (14), as shown in Table 6. After that, these screenshots are fused to generate Image F according to Eqs. (15), and the Image F is standardized according to Table 2 to generate Image S. In this case study, the threshold B_T in Section 3.3 is 153. Then, SevereCM, ModerateCM, SlightCM, NoCCM can be established. Afterwards, an appropriate PCM (congestion) is established for the cost maps to build the CongestionCM, as shown in Table 7.

The screenshots of recommended driving routes at various departure times from Google Maps according to typical data in the past are shown in Fig. 14. Unlike the typical traffic congestion data from Google Maps,

the departure times only can be selected as a certain time of a day in the past. Thus, various departure times from Sunday to Saturday from 30 May 2021 to 5 June 2021 are selected. The detailed data of each image in Fig. 14 can be shown in Table 8, where LT denotes the shortest time, ST denotes the longest time, D denotes the distance, and P denotes the priority. Taking recommended routes at 08:00 Monday, 31/05/2021 from Google Maps as an example, the shortest times, longest times, distances, priorities, start point, end point, recommended routes are shown in Fig. 15. After that, the weights from Table 6 at the same time from Sunday to Saturday are given to the recommended driving routes at various departure times, weighted average values and normalized values of shortest times, longest times, distances, and priorities can be calculated by Eqs. (16)-(23) and the results can be shown in Table 8. Similarly, PCM (ST), PCM (LT), PCM (distance), PCM (priority) can be established, as shown in

Table 9, according to normalized values of shortest times, longest times, distances and priorities and Table 3 to provide appropriate weights for R1CM, R2CM, R3CM, and NRCM to build STCM, LTCM, DistanceCM and PriorityCM. Finally, an appropriate PCM (habit) can be established, as shown in

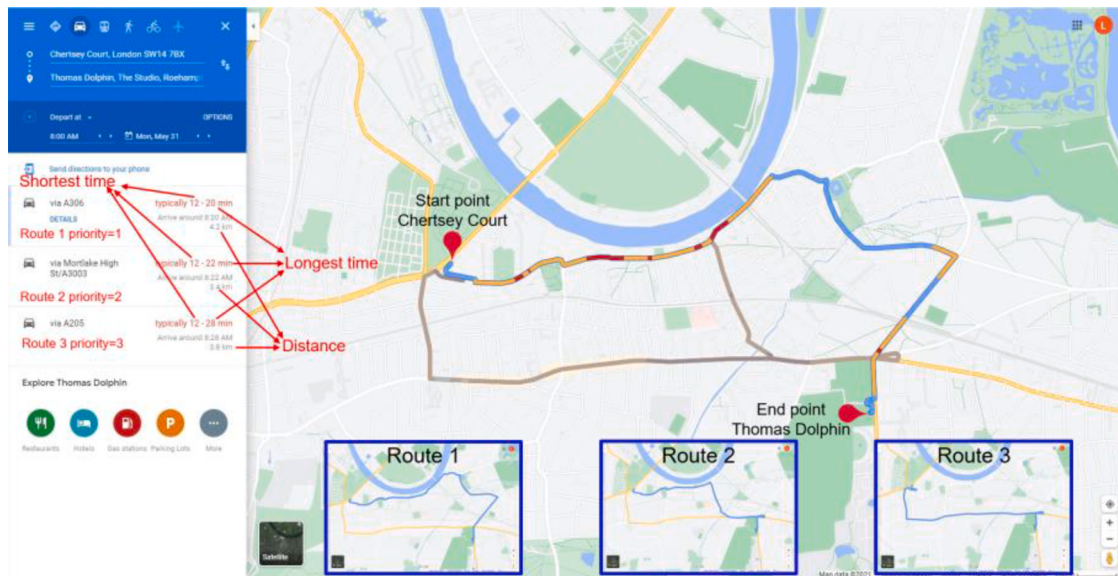
Table 9, to establish the HabitCM.

The screenshots of NO_2 , PM10, PM2.5 and noise distributions in the target area can be shown in Fig. 16. Different colours denote different air

Table 8

Original, weighted average, standardize data of the routes at various times.

08:00 Sunday, 30/05/2021					12:00 Sunday, 30/05/2021					17:00 Sunday, 30/05/2021				
Route	LT	ST	D	P	LT	ST	D	P	LT	ST	D	P		
1	8	14	4.2	1	10	20	4.2	1	9	16	4.2	1		
2	8	14	3.4	3	10	20	3.4	2	9	18	3.4	2		
3	8	14	3.8	2	12	28	3.8	3	10	22	3.8	3		
08:00 Monday, 31/05/2021					12:00 Monday, 31/05/2021				17:00 Monday, 31/05/2021					
Route	LT	ST	D	P	LT	DT	D	P	LT	DT	D	P		
1	12	20	4.2	1	10	18	4.2	1	10	20	4.2	1		
2	12	22	3.4	2	9	18	3.4	2	10	20	3.4	2		
3	12	28	3.8	3	10	22	3.8	3	12	28	3.8	3		
08:00 Tuesday, 01/06/2021					12:00 Tuesday, 01/06/2021				17:00 Tuesday, 01/06/2021					
Route	LT	ST	D	P	LT	DT	D	P	LT	DT	D	P		
1	10	20	4.2	1	10	18	4.2	1	10	20	4.2	1		
2	12	22	3.4	2	9	18	3.4	2	10	20	3.4	2		
3	12	30	3.8	3	10	22	3.8	3	12	28	3.8	3		
08:00 Wednesday, 02/06/2021					12:00 Wednesday, 02/06/2021				17:00 Wednesday, 02/06/2021					
Route	LT	ST	D	P	LT	DT	D	P	LT	DT	D	P		
1	12	22	4.2	1	10	18	4.2	1	10	20	4.2	1		
2	12	22	3.4	2	9	18	3.4	2	10	22	3.4	2		
3	14	35	3.8	3	10	24	3.8	3	12	28	3.8	3		
08:00 Thursday, 03/06/2021					12:00 Thursday, 03/06/2021				17:00 Thursday, 03/06/2021					
Route	LT	ST	D	P	LT	DT	D	P	LT	DT	D	P		
1	10	22	4.2	1	10	18	4.2	1	10	20	4.2	1		
2	12	22	3.4	2	9	18	3.4	2	10	22	3.4	2		
3	14	30	3.8	3	10	24	3.8	3	12	28	3.8	3		
08:00 Friday, 04/06/2021					12:00 Friday, 04/06/2021				17:00 Friday, 04/06/2021					
Route	LT	ST	D	P	LT	DT	D	P	LT	DT	D	P		
1	10	20	4.2	1	10	20	4.2	1	12	24	4.2	1		
2	12	22	3.4	2	10	20	3.4	2	10	24	3.4	2		
3	12	28	3.8	3	12	26	3.8	3	14	30	3.8	3		
08:00 Saturday, 05/06/2021					12:00 Saturday, 05/06/2021				17:00 Saturday, 05/06/2021					
Route	LT	ST	D	P	LT	DT	D	P	LT	DT	D	P		
1	9	14	4.2	1	12	22	4.2	1	10	18	4.2	1		
2	9	14	3.4	3	12	24	3.4	2	10	18	3.4	2		
3	8	16	3.8	2	12	30	3.8	3	12	26	3.8	3		
Weighted average data														
Route	LT	ST	D	P	LT	DT	D	P	LT	DT	D	P		
1	10.404	19.899	4.200	1	0.401	0.281	1.000	0						
2	10.426	20.638	3.400	2.021	0.404	0.316	0.000	0.516						
3	11.844	27.352	3.800	2.979	0.641	0.636	0.500	1						

**Fig. 15.** Recommended routes at 08:00 Monday, 31/05/2021 from Google Maps.

pollutant concentrations and noise levels that can be described in [Table 10](#). PCM (NO₂), PCM (PM10), PCM (PM2.5), and PCM (noise) in [Table 10](#) are employed to make NO₂CM, PM10, PM2.5CM, and NoiseCM, respectively. The tolerance values (T) mentioned in Section 3.5 for

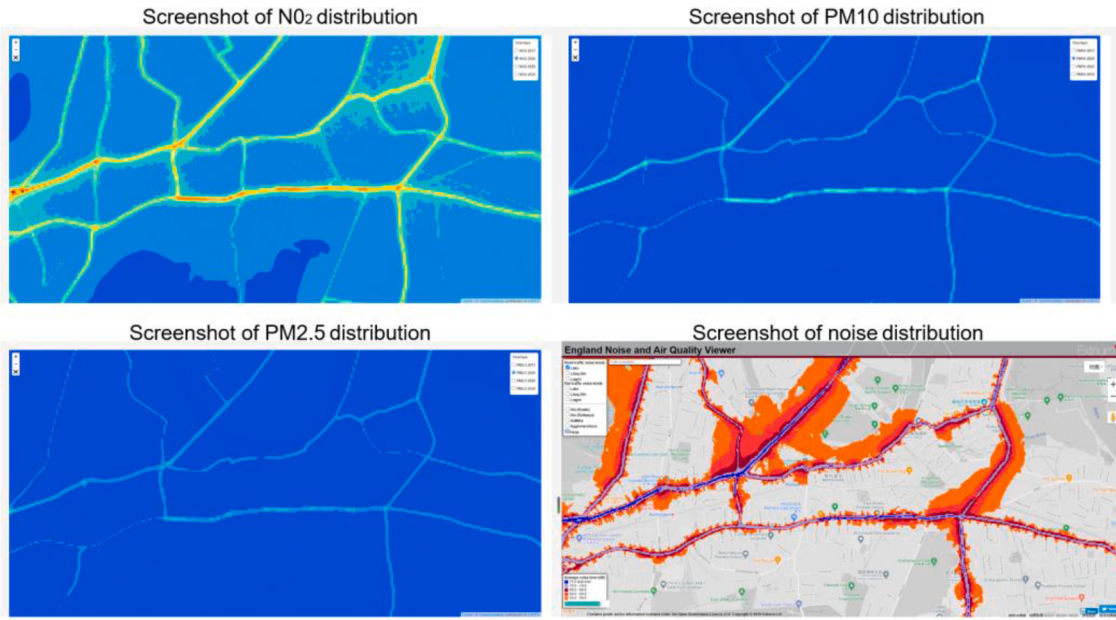
NO₂CM, PM10, PM2.5CM, and NoiseCM are 20, 20, 20, and 10, respectively. PCM (air) and PCM (environment), are employed to make AirCM and EnvironmentCM in [Table 10](#).

After LandCM, CongestionCM, HabitCM, EnvironmentCM are

Table 9

PCM (habit) for the driving route selection habit cost map (HabitCM).

PCM (ST)							PCM (LT)									
Criteria map	R1CM	R2CM	R3CM	NRCM	ω_i	$W(i)$	Criteria map	R1CM	R2CM	R3CM	NRCM	ω_i	$W(i)$			
R1CM	1	1	1/2	1/8	0.101	0.075	R1CM	1	1/2	1/3	1/9	0.070	0.052			
R2CM	1	1	1/2	1/8	0.101	0.075	R2CM	2	1	1/3	1/9	0.099	0.074			
R3CM	2	2	1	1/8	0.171	0.127	R3CM	3	3	1	1/8	0.197	0.147			
NRCM	8	8	8	1	0.975	0.723	NRCM	9	9	8	1	0.973	0.727			
Values	λ_{max}		Consistency ratio		Consistency		Values	λ_{max}		Consistency ratio		Consistency				
Results	4.061		0.0225		Pass		Results	4.183		0.0679		Pass				
PCM (distance)								PCM (priority)								
Criteria map	R1CM	R2CM	R3CM	NRCM	ω_i	$W(i)$	Criteria map	R1CM	R2CM	R3CM	NRCM	ω_i	$W(i)$			
R1CM	1	5	3	1/7	0.240	0.174	R1CM	1	1/3	1/5	1/9	0.059	0.043			
R2CM	1/5	1	1/3	1/9	0.059	0.043	R2CM	3	1	1/3	1/8	0.116	0.084			
R3CM	1/3	3	1	1/8	0.116	0.084	R3CM	5	3	1	1/7	0.240	0.174			
NRCM	7	9	8	1	0.962	0.699	NRCM	9	8	7	1	0.962	0.699			
Values	λ_{max}		Consistency ratio		Consistency		Values	λ_{max}		Consistency ratio		Consistency				
Results	4.262		0.0970		Pass		Results	4.262		0.0970		Pass				
PCM (habit)																
Cost map	STCM		LTCM		DistanceCM		PriorityCM		ω_i		$W(i)$					
STCM	1		3		3		2		0.810		0.455					
LTCM	1/3		1		1		1/2		0.251		0.141					
DistanceCM	1/3		1		1		1/2		0.251		0.141					
PriorityCM	1/2		2		2		1		0.467		0.263					
Values	λ_{max}		Consistency ratio		Consistency		Values	λ_{max}		Consistency ratio		Consistency				
Results	4.010		0.00384		Pass		Results	4.262		0.0970		Pass				

**Fig. 16.** Screenshots of various air pollutants and noise distributions in the target areas.

determined, an appropriate PCM (overall) is established to build the overall cost map (OverallCM). In the target research area, remaining road networks (RRN), some cemeteries, River Thames are set as forbidden zones. Two OverallCMs are established to compare with each other. OverallCM 1 is established according to PCM (overall) 1, as shown in Table 11. OverallCM 2 is established directly by adding forbidden zones into LandCM, which only consider the building demolition and land use factors and ignore the influence of CongestionCM, HabitCM and EnvironmentCM.

4.3. Urban road planning results

The computation process of the cost maps and corresponding PCMs and weights are shown in Fig. 17. The computation method is elaborated

in Section 3 and the original data, PCMs, and weights are shown in Section 4.2. Finally, cost maps are merged by multiplying corresponding weights according to the PCMs to generate new cost maps using Eqs. (11). The cost map results are shown in Fig. 19, and the road planning scheme is generated according to OverallCMs. The road Plan 1, Plan 2 are generated according to OverallCM 1 and OverallCM 2, respectively, as shown in Fig. 18, where the solid lines represent newly built sections, and the dashed lines represent road-widening sections. Plan 1 is 3314.152 m and mainly suggests widening some sections of high-grade roads: A205 and A306. Plan 2 is 2464.729 m which goes through some existing buildings and has several newly built sections and road-widening sections for branch roads. Though Plan 1 is longer than Plan 2, Plan 1 mainly suggests widening the existing main road rather than widening some branch roads or constructing new roads among existing

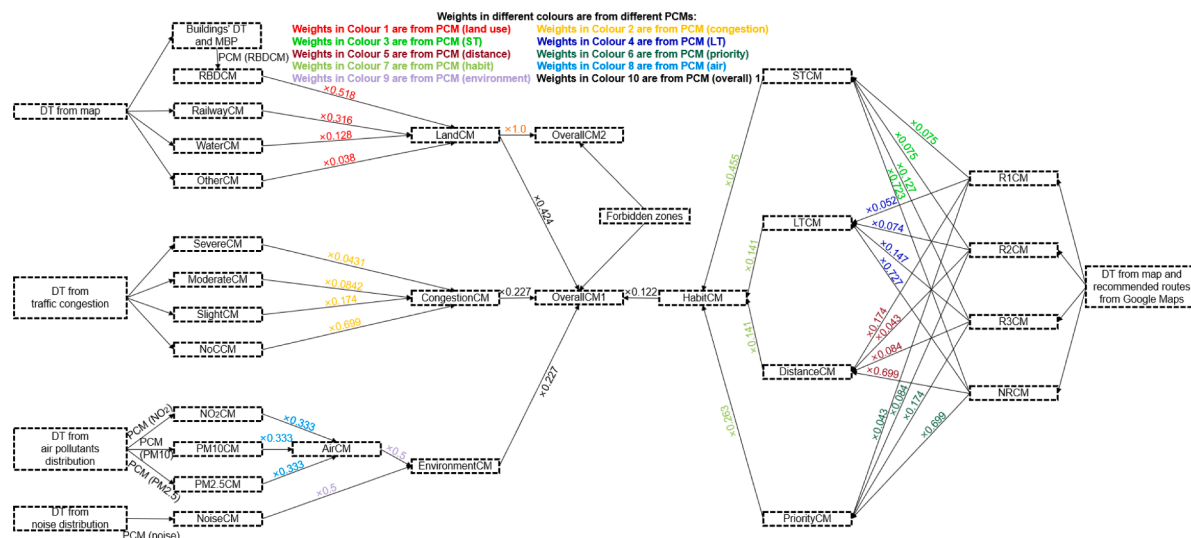
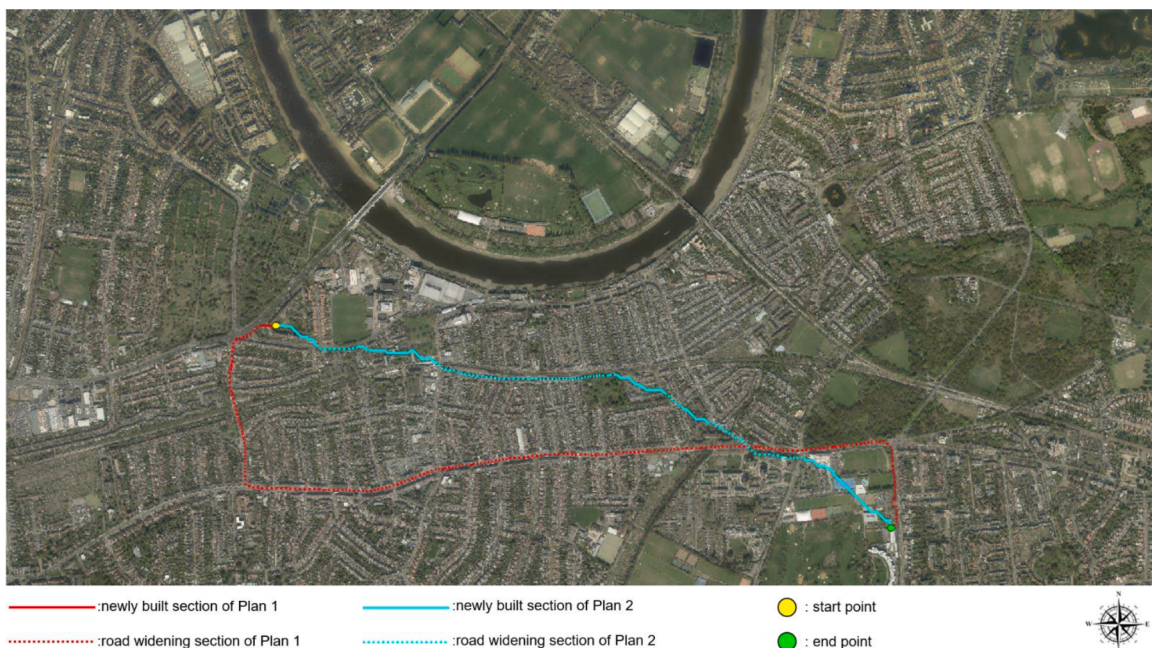
Table 10
PCMs for environmental factors.

PCM (N02)								
Levels	Level 1 1rgb:24,154,23425 ug/ m3rgb:36,208,21228 ug/m3	Level 2 rgb:135,252,20831 ug/m3rgb:112,224,13934 ug/m3	Level 3 rgb:169,236,8937 ug/ m3rgb:255,255,13440 ug/m3	Level 4 rgb:255,216,1343 ug/ m3rgb:255,177,9946 ug/m3	Level 5 5rgb:249,131,1349 ug/m3rgb: 255,13,1352 ug/ m3	Level 6 6rgb:134,13,7455 ug/m3	ω_x	V_x
Level 1	1	2	3	4	5	6	0.764	97.537
Level 2	1/2	1	2	3	4	5	0.500	63.852
Level 3	1/3	1/2	1	2	3	4	0.319	40.693
Level 4	1/4	1/3	1/2	1	2	3	0.201	25.661
Level 5	1/5	1/4	1/3	1/2	1	2	0.128	16.340
Level 6	1/6	1/5	1/4	1/3	1/2	1	0.0855	10.917
Values	λ_{max}		Consistency ratio			Consistency		
Results	6.122		0.0198			Pass		
PCM (PM10)								
Levels	Level 1 rgb:18,82,244 22 ug/m3	Level 2 rgb:23,153,233 25 ug/m3	Level 3 rgb:36,209,211 28 ug/m3	Level 4 rgb:136,253,209 31 ug/m3	Level 5 rgb:112,224,139 34 ug/m3	ω_x	V_x	
Level 1	1	2	3	4	5	0.787	106.728	
Level 2	1/2	1	2	3	4	0.493	66.942	
Level 3	1/3	1/2	1	2	3	0.301	40.780	
Level 4	1/4	1/3	1/2	1	2	0.183	24.800	
Level 5	1/5	1/4	1/3	1/2	1	0.116	15.750	
Values	λ_{max}		Consistency ratio			Consistency		
Results	5.068		0.0152			Pass		
PCM (PM2.5)								
Levels	Level 1 rgb:17,81,243 22 ug/m3	Level 2 rgb:24,154,234 25 ug/m3	Level 3 rgb:34,217,210 28 ug/m3	ω_x	V_x			
Level 1	1	2	3	0.847	137.602			
Level 2	1/2	1	2	0.466	75.7252			
Level 3	1/3	1/2	1	0.256	41.673			
Values	λ_{max}		Consistency ratio			Consistency		
Results	3.009		0.00793			Pass		
PCM (noise)								
Levels	Level 6 other colours <55.0 dB	Level 1 rgb:255,102,0 55.0–59.9dB	Level 2 rgb: 255,51,51 60.0–64.9dB	Level 3 rgb: 153,0,51 65.0–69.9dB	Level 4 rgb: 173,154,214 70.0–74.9dB	Level 5 rgb: 0,0,224 ≥75dB	ω_x	V_x
Level 6	1	2	3	4	5	6	0.764	97.537
Level 1	1/2	1	2	3	4	5	0.500	63.852
Level 2	1/3	1/2	1	2	3	4	0.319	40.693
Level 3	1/4	1/3	1/2	1	2	3	0.201	25.661
Level 4	1/5	1/4	1/3	1/2	1	2	0.128	16.340
Level 5	1/6	1/5	1/4	1/3	1/2	1	0.0855	10.917
Values	λ_{max}		Consistency ratio			Consistency		
Results	6.122		0.0198			Pass		
PCM (air)								
Cost map	NO ₂	PM10	PM2.5	ω_i	ω_i	W(i)	Cost map	Air
NO ₂	1	1	1	1	0.577	0.333	Air	1
PM10	1	1	1	1	0.577	0.333	Noise	1
PM2.5	1	1	1	1	0.577	0.333		
Values	λ_{max}		Consistency ratio			Values		
Results	3		Consistency			Values		
						λ_{max}		
						Consistency ratio		
						Consistency		
						Pass		

Table 11

PCM (overall) 1 for the overall cost map 1 (OverallCM 1).

Cost map	LandCM	CongestionCM	HabitCM	EnvironmentCM	w_i	$W(i)$
LandCM	1	2	3	2	0.777	0.424
CongestionCM	1/2	1	2	1	0.416	0.227
HabitCM	1/3	1/2	1	1/2	0.224	0.122
EnvironmentCM	1/2	1	2	1	0.416	0.227
Values	λ_{max}	Consistency ratio	Consistency			
Results	4.010	0.00384	Pass			

**Fig. 17.** Computation process of cost maps.**Fig. 18.** Urban road planning results.

buildings, which can reduce the impact on citizens' properties, alleviate road congestion, conform to people's driving habits, and consider air pollution and noise factors.

5. Discussion

In Section 4.3, two very different road planning results are exhibited. Plan 2 is shorter and mainly advocates building new roads and widening existing branch roads among the existing buildings, which only considers land use and building demolition. Plan 1 is longer and mainly

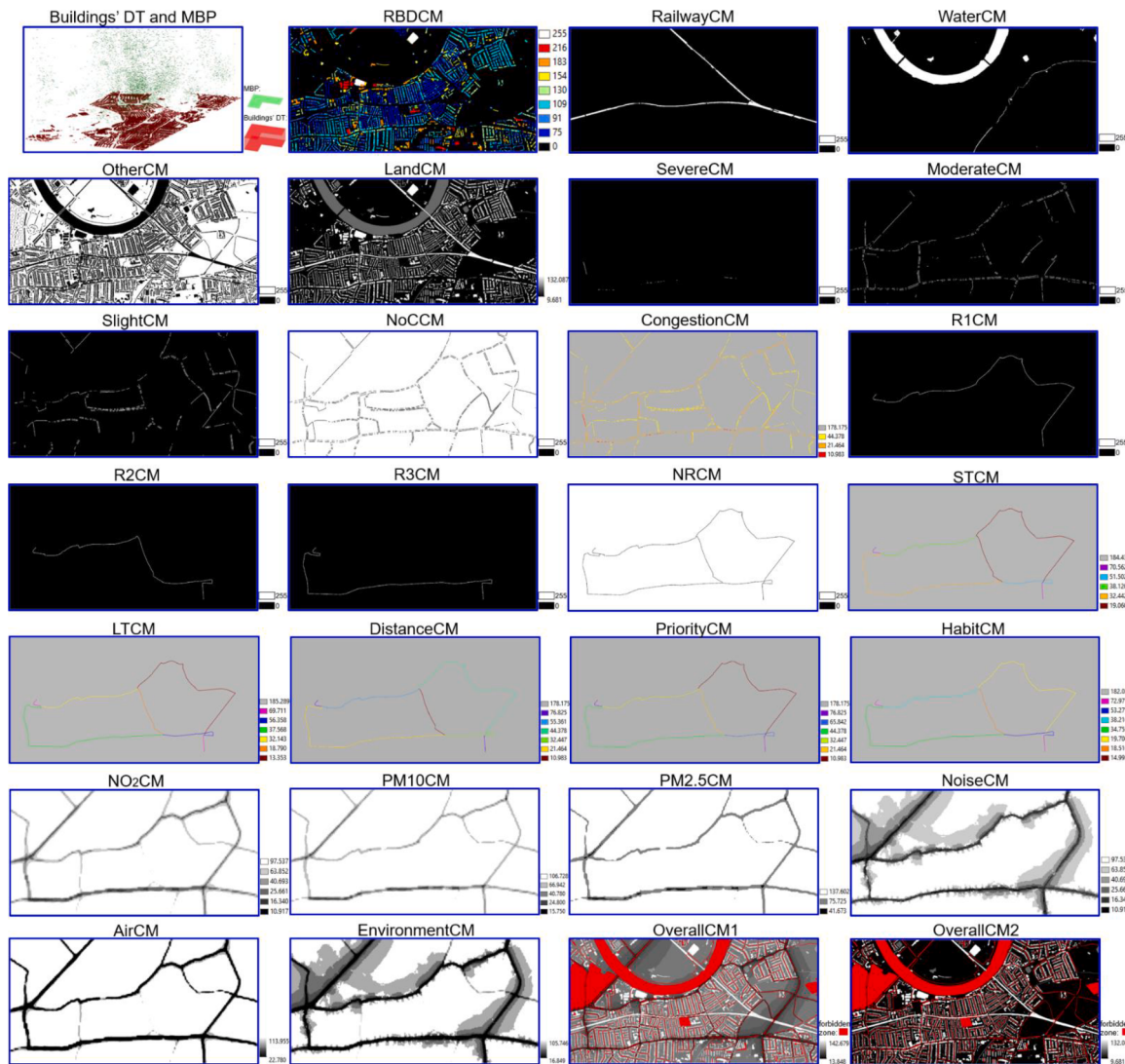


Fig. 19. All cost maps in the case study.

advocates widening existing main roads, considering economic, social, environmental, engineering factors. These factors can be divided into two categories: demands and constraints. On the one hand, urban road planning strives to alleviate traffic congestion and meet other potential demands from the citizens, such as driving route selection habits. On the other hand, urban road planning is limited by economic, social, and environmental constraints, such as building demolition, land use, air quality, and noise.

Compared with Plan 2, Plan 1 proposes a more sustainable result that is functional, economical, people-friendly, and eco-friendly. First, from the perspective of being functional, Plan 1 and Plan 2 both consider how to alleviate traffic congestion by using the limited remaining space in the city. However, Plan 1 digitalizes traffic congestion data to alleviate traffic congestion more purposefully and accurately. Second, from the economic perspective, the proposed methods Plan 1 and Plan 2 both consider reducing building demolition and land-use costs.

Furthermore, the generated road alignment in Plan 1 using the proposed method go through the area with a high concentration of air pollutants and loud noise where there are more vehicles. It can also alleviate traffic congestion and is beneficial to the economy. Third, from the perspective of being people-friendly, Plan 1 considers the driving route selection habits of the citizens and has the trend towards widening the existing main roads which drivers frequently use. In addition, both Plan 1 and Plan 2 reduce the influence of building demolition on citizens

and consider the compensations for the citizens who lose their properties according to the policy. Fourth, from the perspective of being eco-friendly, the road construction based on Plan 1 has the trend to be conducted in the areas with a high concentration of air pollutants and loud noise, which can reduce the influence on the quiet areas with better air quality. Finally, from the engineering perspective, Plan 1 and Plan 2 consider both new road construction and the existing old road widening.

Some studies proposed hybrid MCDM-GIS methods to assist road planning based on cost maps. However, data collection, interpretation and analysis are essential for implementing MCDM to urban road planning, which has not been focused on, while a digital twin can provide data and processed information of existing environments, surroundings, related projects for the MCDM process. Thus, this paper proposes a DT-MCDM-GIS framework for urban road planning to fill the gaps. Compared with Plan 2, Plan 1 employed more digitalisation methods for more sustainable factors.

However, some limitations still exist in this research:

First, the research considers five types of factors. Nevertheless, urban road planning is a very complex interdisciplinary problem that needs to consider more factors such as engineering and economic factors (cut-fill volume, the construction of bridges, intersections and interchanges, occupation and relocation of existing pipelines caused by roads, etc.), social factors (the layout of commercial areas, residential areas, industrial areas, green areas, etc.), environmental factors (destruction of

existing vegetation, the impact on the ecological areas, etc.), historical factors (protection of cultural heritage). However, many of these factors are beyond the scope of this study.

Second, this paper proposed a DT-MCDM-GIS framework mainly based on the AHP method while more MCDM methods, such as TOPSIS, fuzzy AHP, fuzzy TOPSIS, MOORA, SAW, Delphi and ELECTRE can also be implemented. Different MCDM methods have different merits and demerits; a comparison of these methods would be another work done by other researchers (Broniewicz & Ogrodnik, 2020; Dahooie, Mohammadi, & Vanaki, 2019; Zafar, Wuni, Shen, Zahoor, & Xue, 2020). Among these methods, AHP is the most widely used one.

Third, as mentioned in some existing studies (Yakar & Celik, 2014), different projects in cities with different characteristics should employ different PCMs. Therefore, it is impossible to propose omnipotent PCMs for all urban road planning projects. However, this paper aims to introduce a DT-MCDM-GIS framework for urban road planning using AHP as an example rather than focusing on various MCDM methods and PCMs from experts in different domains.

6. Conclusion

This paper proposes a sustainable urban road planning approach based on the DT-MCDM-GIS framework. DT can digitalize the physical world to provide various data for the whole process; MCDM can provide criteria and evaluation methods; GIS can provide an integrated environment for analysis. Economic, social, environmental, and engineering factors are considered for urban road planning to balance the city's constraints and the citizens' demands. The proposed approach can plan urban roads considering both new road construction and existing old road widening. An urban road planning was conducted in southwest London using the proposed approach as a case study.

This research can bring three main contributions to the field. First, this research upgrades the hybrid MCDM-GIS method from digitalization to a DT-MCDM-GIS framework for sustainable urban road planning considering various factors. Various digital twin methods can interpret various data into understandable expressions to assist urban road planning. Second, using the proposed approach, sustainable urban road planning can be realized considering various factors, namely building demolition and land use, traffic congestion, driving route selection habit, air quality, and noise. These factors have not been considered comprehensively in the previous research in urban road planning. Third, most existing studies only consider urban road planning for new road construction. The proposed approach considers both new road construction and existing old road widening.

According to this research and limitations in Section 5, several future study recommendations are presented. First, in addition to building demolition and land use, traffic congestion, driving route selection habits, air quality, and noise, more factors should be considered for sustainable urban road planning. Thus, more digital twinning methods should be studied for various factors to provide multi-type, multi-source, multi-disciplinary data for sustainable urban road planning. Furthermore, in addition to the AHP method, more MCDM methods should be employed and compared under the DT-MCDM-GIS framework, such as TOPSIS, fuzzy AHP, fuzzy TOPSIS, MOORA SAW, Delphi, ELECTRE, etc. Finally, urban road planning is a complex multi-disciplinary problem, and different projects should employ different suitable MCDM methods.

Declaration of Competing Interest

The authors declare that they have no known competing financial interests or personal relationships that could have appeared to influence the work reported in this paper.

Acknowledgments

This study is supported by the Major Science &Technology Project of Hubei (grant no. 2020ACA006)

References

- Addanki, S. C., & Venkataraman, H. (2017). Greening the economy: A review of urban sustainability measures for developing new cities. *Sustainable Cities and Society*, 32, 1–8. <https://doi.org/10.1016/j.scs.2017.03.009>
- Badawi, H. F., Laamarti, F., & Saddik, A. E. (2021). Devising digital twins DNA paradigm for modeling ISO-based city services. *Sensors (Switzerland)*, 21(4), 1–18. <https://doi.org/10.3390/s21041047>
- Beukes, E., Vanderschuren, M., Zuidgeest, M., Brussel, M., & van Maarseveen, M. (2013). Quantifying the contextual influences on road design. *Computer-Aided Civil and Infrastructure Engineering*, 28(5), 344–358. <https://doi.org/10.1111/j.1467-8667.2012.00804.x>
- Brahmantoro, W., Hidayat, S., & Sebayang, N. (2019). Roads widening selection in Tulungagung: Application of AHP. *International Journal of Scientific and Technology Research*, 8(10), 1517–1522. <https://www.ijstr.org/final-print/oct2019/Roads-Widening-Selection-In-Tulungagung-Application-Of-Ahp.pdf>
- Broniewicz, E., & Ogrodnik, K. (2020). Multi-criteria analysis of transport infrastructure projects. *Transportation Research Part D: Transport and Environment*, 83. <https://doi.org/10.1016/j.trd.2020.102351>
- Chen, X., Wang, H. H., & Tian, B. (2019). Visualization model of big data based on self-organizing feature map neural network and graphic theory for smart cities. *Cluster Computing*, 22, 13293–13305. <https://doi.org/10.1007/s10586-018-1848-1>
- Dahooie, J. H., Mohammadi, N., & Vanaki, A. S. (2019). Using a multi-criteria decision making approach to select the optimal freeway rout (case study: Isfahan-Shiraz Freeway). *International Journal of Mathematics in Operational Research*, 15(3), 372–394. <https://doi.org/10.1504/IJMOR.2019.102079>
- Department for Communities and Local Government. (2010). *Compulsory purchase and compensation booklet 4: Compensation to residential owners and occupiers*. Retrieved from https://assets.publishing.service.gov.uk/government/uploads/system/uploads/attachment_data/file/571453/booklet4.pdf.
- EDINA. (2021). Digimap. Retrieved from <https://digimap.edina.ac.uk/lidar>.
- Ehrlich, M. V., Hilber, C. A. L., & Schöni, O. (2018). Institutional settings and urban sprawl: Evidence from Europe. *Journal of Housing Economics*, 42, 4–18. <https://doi.org/10.1016/j.jhe.2017.12.002>
- Extrium. (2017). England Noise and Air Quality Viewer. Retrieved from <http://www.extrium.co.uk/noiseviewer.html>.
- Fernandes, P., Tomás, R., Acuto, F., Pascale, A., Bahmankhah, B., Guarnaccia, C., et al. (2020). Impacts of roundabouts in suburban areas on congestion-specific vehicle speed profiles, pollutant and noise emissions: An empirical analysis. *Sustainable Cities and Society*, 62. <https://doi.org/10.1016/j.scs.2020.102386>
- Francini, M., Gaudio, S., Palermo, A., & Viapiana, M. F. (2020). A performance-based approach for innovative emergency planning. *Sustainable Cities and Society*, 53. <https://doi.org/10.1016/j.scs.2019.101906>
- Gipps, P. G., Gu, K. Q., Held, A., & Barnett, G. (2001). New technologies for transport route selection. *Transportation Research Part C: Emerging Technologies*, 9(2), 135–154. [https://doi.org/10.1016/S0968-090X\(00\)00040-1](https://doi.org/10.1016/S0968-090X(00)00040-1)
- Grieves, M., & Vickers, J. (2016). Digital twin: Mitigating unpredictable, undesirable emergent behavior in complex systems. *Transdisciplinary Perspectives on Complex Systems: New Findings and Approaches*, 85–113. https://doi.org/10.1007/978-3-319-38756-7_4
- Grossardt, T., Bailey, K., & Brumm, J. (2001). Analytic minimum impedance surface: Geographic information system-based corridor planning methodology. *Transportation Research Record: Journal of the Transportation Research Board*, 1758(1), 224–232. <https://doi.org/10.3141/1768-26>
- HM Land Registry Open Data. (2021). UK House Price Index. Retrieved from <https://landregistry.data.gov.uk/app/ukhpi/browse?from=2020-04-01&location=http%3A%2F%2Flandregistry.data.gov.uk%2Fid%2Fregion%2Fhounslow&to=2021-04-01&lang=en>.
- Hosseini, S. A. O., Moghadasi, P., & Fallah, A. (2019). Forest road network design based on multipurpose forestry management in hyrcanian forest. *Journal of Environmental Science and Management*, 22(2), 13–20. <https://ovcre.uplb.edu.ph/journals-uplb/index.php/JESAM/article/view/169/151>
- Hou, S., Maruyama, N., Hirota, M., & Kato, S. (2009). Optimization framework for road network directed by unblocked reliability for given network topology and inelastic demand with stochastic user equilibrium. *WSEAS Transactions on Business and Economics*, 6(6), 292–301. <https://citeserx.ist.psu.edu/viewdoc/download?doi=10.1.1.576.8857&rep=rep1&type=pdf>
- Imperial College London. (2021). London Air. Retrieved from <https://www.londonair.org.uk/london/aspx/futuremaps.asp>.
- Jiang, F., Ma, L., Broyd, T., & Chen, K. (2021). Digital twin and its implementations in the civil engineering sector. *Automation in Construction*, 130. <https://doi.org/10.1016/j.autcon.2021.103838>
- Kabisch, N., & Haase, D. (2013). Green spaces of European cities revisited for 1990–2006. *Landscape and Urban Planning*, 110(1), 113–122. <https://doi.org/10.1016/j.landurbplan.2012.10.017>
- Khayamini, R., Shetab-Boushehr, S. N., Hosseini, S. M., & Karimi, H. (2020). A sustainable approach for selecting and timing the urban transportation infrastructure projects in large-scale networks: A case study of Isfahan. *Iran Sustainable Cities and Society*, 53. <https://doi.org/10.1016/j.scs.2019.101981>

- Lanqin, X. (2020). Intelligent multimedia urban planning Construction based on spectral clustering algorithms of large data mining. *Multimedia Tools and Applications*, 79 (47–48), 35183–35194. <https://doi.org/10.1007/s11042-019-7572-x>
- Leng, J., Wang, D., Shen, W., Li, X., Liu, Q., & Chen, X. (2021). Digital twins-based smart manufacturing system design in Industry 4.0: A review. *Journal of Manufacturing Systems*, 60, 119–137. <https://doi.org/10.1016/j.jmsy.2021.05.011>
- Liu, S., Bao, J., Lu, Y., Li, J., Lu, S., & Sun, X. (2021). Digital twin modeling method based on biomimicry for machining aerospace components. *Journal of Manufacturing Systems*, 58, 180–195. <https://doi.org/10.1016/j.jmsy.2020.04.014>
- Ma, C. X., & Peng, F. L. (2021). Monetary evaluation method of comprehensive benefits of complex underground roads for motor vehicles orienting urban sustainable development. *Sustainable Cities and Society*, 65. <https://doi.org/10.1016/j.scs.2020.102569>
- Marcucci, E., Gatta, V., Pira, M. Le, Hansson, L., & Bråthen, S. (2020). Digital twins: A critical discussion on their potential for supporting policy-making and planning in urban logistics. *Sustainability (Switzerland)*, 12(24), 1–15. <https://doi.org/10.3390/su122410623>
- Meng, M., & Shao, C. F. (2011). DEA and TOPSIS combination model for the construction scheduling of urban road projects. In *2011 International Conference on Transportation, Mechanical, and Electrical Engineering*. TMEE. <https://doi.org/10.1109/TMEE.2011.6199593>, 2011, 1937–1940.
- Ng, C. P., Law, T. H., Jakarni, F. M., & Kulanthayan, S. (2018). Relative improvements in road mobility as compared to improvements in road accessibility and urban growth: A panel data analysis. *Transportation Research Part A: Policy and Practice*, 117, 292–301. <https://doi.org/10.1016/j.tra.2018.08.032>
- O'Dwyer, E., Pan, I., Charlesworth, R., Butler, S., & Shah, N. (2020). Integration of an energy management tool and digital twin for coordination and control of multi-vector smart energy systems. *Sustainable Cities and Society*, 62. <https://doi.org/10.1016/j.scs.2020.102412>
- Office for National Statistics. (2017). House prices: How much does one square metre cost in your area?. Retrieved from <https://www.ons.gov.uk/peoplepopulationandcommunity/housing/articles/housepriceshowmuchdoesonesquaremetrecostinyourarea/2017-10-11.pdf>.
- Old Oak and Park Royal Development Corporation. (2018). Tall Buildings Statement. Retrieved from https://www.london.gov.uk/sites/default/files/52_tall_buidings_statement_2018.pdf.
- Ouma, Y. O., Yabann, C., Kirichu, M., & Tateishi, R. (2014). Optimization of urban highway bypass horizontal alignment: A methodological overview of intelligent spatial mcdm approach using fuzzy ahp and gis. *Advances in Civil Engineering*. <https://doi.org/10.1155/2014/182568>, 2014.
- Pucher, J., Peng, Z. R., Mittal, N., Zhu, Y., & Korattyswaroopam, N. (2007). Urban transport trends and policies in China and India: Impacts of rapid economic growth. *Transport Reviews*, 27(4), 379–410. <https://doi.org/10.1080/01441640601089988>
- Saaty, T. L. (1977). A scaling method for priorities in hierarchical structures. *Journal of Mathematical Psychology*, 15(3), 234–281. [https://doi.org/10.1016/0022-2496\(77\)90033-5](https://doi.org/10.1016/0022-2496(77)90033-5)
- Saaty, T. L. (1990). How to make a decision: The analytic hierarchy process. *European Journal of Operational Research*, 48(1), 9–26. [https://doi.org/10.1016/0377-2217\(90\)90057-1](https://doi.org/10.1016/0377-2217(90)90057-1)
- Schislyayeva, E. R., & Kovalenko, E. A. (2021). Innovations in logistics networks on the basis of the digital twin. *Academy of Strategic Management Journal*, 20(SpecialIssue2), 1–17. <https://www.abacademies.org/articles/innovations-in-logistics-networks-on-the-basis-of-the-digital-twin.pdf>.
- Schrötter, G., & Hürzeler, C. (2020). The Digital Twin of the City of Zurich for Urban Planning. *PFG - Journal of Photogrammetry, Remote Sensing and Geoinformation Science*, 88(1), 99–112. <https://doi.org/10.1007/s41064-020-00092-2>
- Scoppa, M., Bawazir, K., & Alawadi, K. (2018). Walking the superblocs: Street layout efficiency and the sikkak system in Abu Dhabi. *Sustainable Cities and Society*, 38, 359–369. <https://doi.org/10.1016/j.scs.2018.01.004>
- Shahat, E., Hyun, C. T., & Yeom, C. (2021). City digital twin potentials: A review and research agenda. *Sustainability (Switzerland)*, 13(6), 3386. <https://doi.org/10.3390/su13063386>
- Singh, M. P., Singh, P., & Singh, P. (2019). Fuzzy AHP-based multi-criteria decision-making analysis for route alignment planning using geographic information system (GIS). *Journal of Geographical Systems*, 21(3), 395–432. <https://doi.org/10.1007/s10109-019-00296-0>
- Tao, F., Zhang, H., Liu, A., & Nee, A. Y. C. (2019). Digital Twin in Industry: State-of-the-Art. *IEEE Transactions on Industrial Informatics*, 15(4), 2405–2415. <https://doi.org/10.1109/TII.2018.2873186>
- Wang, X., & Chen, Y. (2016). A novel hybrid algorithm to optimize travel paths in cities. *International Journal of Simulation: Systems, Science and Technology*, 17(45). <https://doi.org/10.5013/IJSSST.a.17.45.20>, 20.21–20.25.
- White, G., Zink, A., Codecá, L., & Clarke, S. (2021). A digital twin smart city for citizen feedback. *Cities*, 110. <https://doi.org/10.1016/j.cities.2020.103064>
- Yakar, F., & Celik, F. (2014). A highway alignment determination model incorporating GIS and Multi-Criteria Decision Making. *KSCE Journal of Civil Engineering*, 18(6), 1847–1857. <https://doi.org/10.1007/s12205-014-0130-1>
- Zafar, I., Wuni, I. Y., Shen, G. Q., Zahoor, H., & Xue, J. (2020). A decision support framework for sustainable highway alignment embracing variant preferences of stakeholders: Case of China Pakistan economic corridor. *Journal of Environmental Planning and Management*, 63(9), 1550–1584. <https://doi.org/10.1080/09640568.2019.1672524>
- Zeng, C., Song, Y., Cai, D., Hu, P., Cui, H., Yang, J., et al. (2019). Exploration on the spatial spillover effect of infrastructure network on urbanization: A case study in Wuhan urban agglomeration. *Sustainable Cities and Society*, 47. <https://doi.org/10.1016/j.scs.2019.101476>
- Zhang, S. (2016). Urban planning based on the optimization-layout of urban logistics network. *Open House International*, 41(3), 124–129. <https://doi.org/10.1108/OHI-03-2016-B0022>